

Neutrino-Electron Scattering: General Constraints on Z' and Dark Photon Models

Manfred Lindner,^a Farinaldo S. Queiroz,^b Werner Rodejohann,^a Xun-Jie Xu^a

^aMax-Planck-Institut für Kernphysik, Saupfercheckweg 1, 69117 Heidelberg, Germany

^bInternational Institute of Physics, Federal University of Rio Grande do Norte, Campus Universitário, Lagoa Nova, Natal-RN 59078-970, Brazil

E-mail: manfred.lindner@mpi-hd.mpg.de, farinaldo.queiroz@iip.ufrn.br,
werner.rodejohann@mpi-hd.mpg.de, xunjie@mpi-hd.mpg.de

Abstract. We study the framework of $U(1)_X$ models with kinetic mixing and/or mass mixing terms. We give general and exact analytic formulas and derive limits on a variety of $U(1)_X$ models that induce new physics contributions to neutrino-electron scattering, taking into account interference between the new physics and Standard Model contributions. Data from TEXONO, CHARM-II and GEMMA are analyzed and shown to be complementary to each other to provide the most restrictive bounds on masses of the new vector bosons. In particular, we demonstrate the validity of our results to dark photon-like as well as light Z' models.

Contents

1	Introduction	1
2	General $U(1)_X$ Models	2
3	Neutrino-Electron Scattering in $U(1)_X$ Models	7
4	Data Fitting	10
5	Bounds	13
6	Conclusion	16
A	Gauge Boson Mass Generation	16
B	Cross Sections of Neutrino-Electron Scattering	18
C	Partial Cross Section	23

1 Introduction

The Standard Model provides an elegant and successful explanation to the electroweak and strong interactions in nature [1]. However, there are many open problems that require physics beyond the Standard Model (SM) to take place. A common particle in these models beyond the SM is a neutral gauge boson, usually referred to as Z' . Such gauge bosons arise naturally in Abelian gauge groups or in gauge groups that embed an Abelian symmetry. The mass of this boson can be generated in several ways, for instance via spontaneous symmetry breaking of a scalar which is singlet or doublet under the SM group, each case leading to very different phenomenology [2]. The mass and interaction strength of Z' bosons with SM particles are very model dependent and entitled to a rich phenomenology from low to high energy scales [3, 4]. Phenomenological studies have been conducted, among others, in the context of colliders [5–18], electroweak precision [19, 20], flavor physics [21–23] or neutrinoless double beta decay [24].

Another particle often present in a multitude of beyond the Standard Model frameworks is the dark photon. Dark photons are typically defined as light vector bosons that possess small kinetic mixing with the QED field strength tensor [25–28]. They are supposed to be much lighter than 90 GeV, the mass of the Z boson. Such particles have also been subject of intense searches at low energy colliders and accelerators [29–47]. We emphasize that when we refer to the Z' mass in our work, we mean the gauge boson mass in a general way, because the Z' can take the form of a dark photon-like boson. The main difference between these two bosons is the type of interactions they

feature with the SM particles. If the kinetic mixing with the QED field strength tensor was the only new term, then the dark photon would only have vectorial interactions with quarks and charged leptons and none whatsoever with the SM neutrinos. In complete dark photon-like models, however, there should be an underlying new broken gauge symmetry, under which SM particles possibly have non-zero charges. Therefore, there could be a mass mixing term in addition to the kinetic mixing, and we arrive again at the classical notion of a Z' boson. For historical reason, Z' models and dark photon models are usually described in different contexts but they simply refer to a massive gauge boson coming from a new gauge symmetry. Therefore, in what follows, we will use the terms Z' and dark photon interchangeably.

Phenomenological studies in the context of Z' or dark photon models in a general setup should include the presence of both mass and kinetic mixing between the vector bosons in the theory. In this work, we provide a general formalism to treat these models. In what regards phenomenology, we will be focused primarily on neutrino-electron scattering process [48–55] since both Z' as well as dark photon-like models give rise to sizable new physics contributions, allowing us to place restrictive constraints.

The observation of neutrino-electron scattering has proven to be an amazing laboratory to test the SM and probe new physics effects motivating a multitude of studies [56–63]. In particular, precise measurements of the neutrino-electron scattering have furnished relevant bounds on Z' bosons for specific models based on the baryon minus lepton number ($B - L$) [64], $L_\mu - L_\tau$ symmetries [65–67] and dark photon-like models [68, 69]. In the future, more measurements will be coming up, see e.g. Refs. [70, 71]. Motivated by the popularity of Z' and dark photon models in the literature and the relevance of neutrino-electron scattering constraints for light dark species we build here up a general setting where constraints using data from neutrino-electron scattering can be placed on Z' and dark photon models in the presence of mass and kinetic mixing terms.

The paper is build up as follows: In Section 2 we develop the general formalism to describe kinetic and mass mixing with of a general Z' with the SM. Exact analytical expressions are provided. Section 3 derives the interactions relevant for neutrino-electron scattering and gives expressions for cross sections. The fitting procedure is described in Sec. 4, bounds on the masses and couplings from TEXONO, CHARM-II and GEMMA data are discussed in Section 5, before we conclude in Section 6. Various technical details and lengthy analytical expressions are delegated to appendices.

2 General $U(1)_X$ Models

The formalism for $Z - Z'$ mixing has been frequently discussed in the literature, see e.g. [72]¹. Here we develop the framework in our notation and give exact expressions without any approximation.

¹An analysis for $Z-Z'-Z''$ mixing was performed in [73].

In the presence of the gauge groups $SU(2)_L \times U(1)_Y \times U(1)_X$, the gauge bosons are denoted as \hat{W}_a ($a = 1, 2, 3$), \hat{B} and \hat{X} , respectively. The Lagrangian can be written as

$$\begin{aligned} \mathcal{L} = & -\frac{1}{4}\hat{W}_{\mu\nu}\hat{W}^{\mu\nu} - \frac{1}{4}\hat{B}_{\mu\nu}\hat{B}^{\mu\nu} - \frac{1}{4}\hat{X}_{\mu\nu}\hat{X}^{\mu\nu} - \frac{\epsilon}{2}\hat{B}_{\mu\nu}\hat{X}^{\mu\nu} \\ & + \sum_f \bar{f}i\gamma^\mu D_\mu f + \sum_\phi |D_\mu\phi|^2 \\ & + \text{scalar potential} + \text{Yukawa int.} \end{aligned} \quad (2.1)$$

Here $f = (\nu_L, e_L)^T$, e_R, ν_R, \dots stands for all chiral fermions in the model and ϕ stands for all scalar bosons. Since we are considering the most general case, the fermion and scalar contents are not necessarily the same as in the SM. For example, f may include right-handed neutrinos ν_R ; the scalar sector may contain more than one Higgs doublet or singlets. The covariant derivative is given by

$$D_\mu = \partial_\mu + ig \sum_{a=1}^3 t^a \hat{W}_\mu^a + ig' \frac{Q_Y}{2} \hat{B}_\mu + ig_X \frac{Q_X}{2} \hat{X}_\mu, \quad (2.2)$$

where $t^a = \sigma^a/2$ are the generators of $SU(2)$, g_X is the gauge coupling of the new $U(1)_X$ and $Q_{X,Y}$ are the operators projecting the charges of the particles under $U(1)_X$ and $U(1)_Y$. The two $U(1)$ gauge bosons \hat{B} and \hat{X} couple to each other via the term $\frac{\epsilon}{2}\hat{B}_{\mu\nu}\hat{X}^{\mu\nu}$, which induces kinetic mixing of \hat{X} with the other gauge bosons. This term is essentially guaranteed since it is generated at loop-level even if zero at some scale [74], if there are particles charged under hypercharge and $U(1)_X$. The mass mixing requires that there is a scalar that is charged under the SM and the $U(1)_X$ groups. It is thus absent if the $U(1)_X$ is broken by SM singlet scalars.

The fact that the $U(1)_X$ and the $SU(2)_L \times U(1)_Y$ are broken gauge symmetries leads to mass terms for the gauge bosons as well to mass mixing terms. Appendix A shows the structure of those terms for an arbitrary number of singlet and doublet fields in the realistic scenario in which $U(1)_{\text{em}}$ remains unbroken, see Eqs. (A.11) and (2.9).

We would like to comment here that in the exact physical basis where all gauge bosons have canonical kinetic terms and are mass eigenstates, the mixings mentioned above will be completely removed and converted to corrections to the gauge-fermion or gauge-scalar interactions. Next, we shall show this explicitly. The equations in this section are exact, without any approximation such as $\epsilon \ll 1$ or $g_X \ll 1$.

We define three bases for the corresponding gauge bosons:

- Fundamental basis, which is defined as the basis we start with in Eq. (2.1); gauge bosons are denoted as

$$\hat{\mathbf{X}} \equiv (\hat{W}_1, \hat{W}_2, \hat{W}_3, \hat{B}, \hat{X})^T; \quad (2.3)$$

- Intermediate basis, where the gauge bosons have canonical kinetic terms but a non-diagonal mass matrix, denoted as

$$\mathbf{X} \equiv (W_1, W_2, W_3, B, X)^T; \quad (2.4)$$

- Physical basis, where gauge bosons are mass eigenstates with canonical kinetic terms, denoted as²

$$\mathbf{Z} \equiv (W_1, W_2, A, Z, Z')^T. \quad (2.5)$$

The three bases can be transformed to each other by

$$\mathbf{X} = L_\epsilon^T \hat{\mathbf{X}}, \quad \mathbf{Z} = U^T \mathbf{X}, \quad (2.6)$$

where L_ϵ is a non-unitary linear transformation while U is a unitary transformation, which will be derived below.

First, the kinetic terms in the first row of Eq. (2.1) can be regarded as quadratic-form functions of $\hat{\mathbf{X}}$ (here we can ignore the cubic and quartic terms of non-Abelian gauge bosons),

$$\hat{\mathbf{X}}^T \begin{pmatrix} I_{3 \times 3} & 0 & 0 \\ 0 & 1 & \epsilon \\ 0 & \epsilon & 1 \end{pmatrix} \hat{\mathbf{X}} = \hat{\mathbf{X}}^T L_\epsilon \begin{pmatrix} I_{3 \times 3} & 0 & 0 \\ 0 & 1 & 0 \\ 0 & 0 & 1 \end{pmatrix} L_\epsilon^T \hat{\mathbf{X}} = \mathbf{X}^T \begin{pmatrix} I_{3 \times 3} & 0 & 0 \\ 0 & 1 & 0 \\ 0 & 0 & 1 \end{pmatrix} \mathbf{X}. \quad (2.7)$$

In the second step we have diagonalized the matrix by L_ϵ , given as follows³:

$$L_\epsilon = \begin{pmatrix} I_{3 \times 3} & 0 & 0 \\ 0 & 1 & 0 \\ 0 & \epsilon & \sqrt{1 - \epsilon^2} \end{pmatrix}. \quad (2.8)$$

Eq. (2.7) implies that after the transformation $\hat{\mathbf{X}} \rightarrow \mathbf{X} = L_\epsilon^T \hat{\mathbf{X}}$, the kinetic terms become canonical.

Next we shall diagonalize the mass matrix of gauge bosons. Although the mass matrix depends on details of the scalar sector, such as the numbers or types of new scalars introduced, we show in the appendix that as long as these scalars do not break the $U(1)_{\text{em}}$ symmetry, the mass matrix in the fundamental basis is always block diagonal of the form $\text{diag}(m_W^2, m_W^2, \hat{M}_{3 \times 3})$. Moreover, $\hat{M}_{3 \times 3}$ can be further block-diagonalized into

$$\hat{M}_{3 \times 3} = U_W \begin{pmatrix} 0 & 0 & 0 \\ 0 & z & \delta \\ 0 & \delta & x \end{pmatrix} U_W^T \quad (2.9)$$

²Although (W_1, W_2) are mass eigenstates with the same mass m_W^2 , in the SM they are conventionally converted to $W^\pm = \frac{1}{\sqrt{2}}(W_1 \mp iW_2)$. In this paper, the (W_1, W_2) or W^\pm sector is exactly the same as in the SM. When discussing the bases, we still use (W_1, W_2) for simplicity; later in the charged-current interactions we use W^\pm . The conversion is the same as in the SM.

³Note that L_ϵ is not unique, e.g. one can also use $\begin{pmatrix} I_{3 \times 3} & 0 & 0 \\ 0 & \sqrt{1 - \epsilon^2} & \epsilon \\ 0 & 0 & 1 \end{pmatrix}$ to achieve the transformation from \mathbf{X} to $\hat{\mathbf{X}}$. Actually this transformation can be any matrix of the form $L_\epsilon O_5$ where O_5 is a 5×5 orthogonal matrix.

by the Weinberg rotation

$$U_W = \begin{pmatrix} s_W & c_W & 0 \\ c_W & -s_W & 0 \\ 0 & 0 & 1 \end{pmatrix}, \quad (2.10)$$

where $s_W = \sin \theta_W$, $c_W = \cos \theta_W$. In the above expression for $\hat{M}_{3 \times 3}$, the parameters z, δ and x are related to mass mixing and exact formulas are given in Appendix A. In the intermediate basis, according to Eq. (2.6), the mass matrix is

$$M_{3 \times 3} = L_\epsilon^{-1} \hat{M}_{3 \times 3} (L_\epsilon^T)^{-1}. \quad (2.11)$$

A useful result which can be verified by simple calculation is that the product $M_{3 \times 3}(s_W, c_W, 0)^T$ is zero. It implies that $(s_W, c_W, 0)^T$ is one of the eigenvectors of $M_{3 \times 3}$, which significantly simplifies the diagonalisation process of $M_{3 \times 3}$. The other two eigenvectors should be orthogonal to this one and can be parametrized by an angle α . So all three eigenvectors are given by the columns of the matrix

$$U = \begin{pmatrix} s_W & c_W c_\alpha & c_W s_\alpha \\ c_W & -c_\alpha s_W & -s_W s_\alpha \\ 0 & -s_\alpha & c_\alpha \end{pmatrix}, \quad (2.12)$$

where $s_\alpha = \sin \alpha$ and $c_\alpha = \cos \alpha$. One can use U to diagonalize $M_{3 \times 3}$:

$$M_{3 \times 3} = U \text{diag}(0, m_Z^2, m_{Z'}^2) U^T. \quad (2.13)$$

Here m_Z and $m_{Z'}$ are the masses of the physical gauge bosons with canonical kinetic and mass terms, they are explicitly given in Eqs. (A.15) and (A.16). The solution of α in terms of $\delta, \epsilon, m_{Z'}^2$ and m_Z^2 turns out to be

$$\tan \alpha = \frac{\sqrt{(1 - \epsilon^2)(m_Z^2 - m_{Z'}^2)^2 - 4(\delta + \epsilon m_Z^2 s_W)(\delta + \epsilon s_W m_{Z'}^2)} + \sqrt{1 - \epsilon^2}(m_{Z'}^2 - m_Z^2)}{2(\delta + \epsilon s_W m_{Z'}^2)}, \quad (2.14)$$

which has the following limit if $\epsilon \rightarrow 0$ and $\delta \rightarrow 0$:

$$\tan \alpha = \frac{\delta + \epsilon m_Z^2 s_W}{m_{Z'}^2 - m_Z^2} + \mathcal{O}(\epsilon^2, \delta^2). \quad (2.15)$$

Eq. (2.13) implies that the transformation from the intermediate basis to the physical basis is given by $\mathbf{X} \rightarrow \mathbf{Z} = U^T \mathbf{X}$.

In summary, the gauge bosons mass terms in the three bases are given by

$$\mathcal{L}_{\text{mass}} = \frac{1}{2} \hat{\mathbf{X}}^T \begin{pmatrix} m_W^2 I_{2 \times 2} & \\ & \hat{M}_{3 \times 3} \end{pmatrix} \hat{\mathbf{X}} = \frac{1}{2} \mathbf{X}^T \begin{pmatrix} m_W^2 I_{2 \times 2} & \\ & M_{3 \times 3} \end{pmatrix} \mathbf{X} = \frac{1}{2} \mathbf{Z}^T \begin{pmatrix} m_W^2 I_{2 \times 2} & & \\ & 0 & \\ & & m_Z^2 \\ & & & m_{Z'}^2 \end{pmatrix} \mathbf{Z}. \quad (2.16)$$

Now that we have the transformations between the three bases, we are ready to derive the gauge-fermion interactions in the physical basis.

Note that the transformations represented by L_ϵ and U in Eqs. (2.8) and (2.12) are only limited to the lower 3×3 block. Therefore the charged current interaction mediated by the W^\pm bosons is the same as in the SM. We only need to consider the interactions of fermions with the remaining three gauge bosons, namely \hat{W}_μ^3 , \hat{B}_μ , and \hat{X}_μ in the fundamental basis or A , Z , and Z' in the physical basis. Using Eq. (2.2) these interactions are obtained from

$$\mathcal{L}_{fAZZ'} = \bar{f}\gamma^\mu \left(gt^3 \hat{W}_\mu^3 + g' \frac{Q_Y}{2} \hat{B}_\mu + g_X \frac{Q_X}{2} \hat{X}_\mu \right) f.$$

Here t^3 , Q_Y and Q_X depend on the representation of f in the gauge groups. To proceed with the analysis, we change somewhat the notation and disassemble the $SU(2)$ doublets of fermions and regard t_3 as a quantum number rather than a Pauli matrix. For example, when f is ν_L or e_L , t^3 takes the values $1/2$ or $-1/2$, respectively. In this sense, $(gt^3, g' \frac{Q_Y}{2}, g_X \frac{Q_X}{2})$ can be treated as a vector of numbers rather than 2×2 matrices. Therefore, the interactions in the basis of A , Z , and Z' can be derived by

$$\mathcal{L}_{fAZZ'} = \bar{f}\gamma^\mu \left(\hat{W}_\mu^3, \hat{B}_\mu, \hat{X}_\mu \right) \begin{pmatrix} gt^3 \\ g' Q_Y/2 \\ g_X Q_X/2 \end{pmatrix} f = \bar{f}\gamma^\mu (A, Z, Z') U^T L_\epsilon^{-1} \begin{pmatrix} gt^3 \\ g' Q_Y/2 \\ g_X Q_X/2 \end{pmatrix} f,$$

where $U^T L_\epsilon^{-1}$ is obtained according to Eq. (2.6). Taking the expressions of L_ϵ and U in Eqs. (2.8, 2.12), we get⁴

$$\mathcal{L}_{fAZZ'} = -J_{\text{em}}^\mu A_\mu - J_Z^\mu Z_\mu - J_{Z'}^\mu Z'_\mu, \quad (2.17)$$

$$J_Z^\mu = g c_\alpha J_{\text{NC}}^\mu - s_\alpha J_X^\mu, \quad (2.18)$$

$$J_{Z'}^\mu = g s_\alpha J_{\text{NC}}^\mu + c_\alpha J_X^\mu, \quad (2.19)$$

where J_{em}^μ and J_{NC}^μ are the electromagnetic and neutral currents in the SM respectively, and J_X^μ is a new current which we will refer to as the X -current. For the convenience of later use, we explicitly write them down:

$$\begin{aligned} J_{\text{em}}^\mu &= g s_W \sum_f \bar{f}\gamma^\mu Q_{\text{em}}^f f \\ &= g s_W [e_L \gamma^\mu (-1) e_L + e_R \gamma^\mu (-1) e_R + \dots], \end{aligned} \quad (2.20)$$

$$\begin{aligned} J_{\text{NC}}^\mu &= g \sum_f \bar{f}\gamma^\mu \left[c_W Q_{\text{em}}^f - \frac{Q_Y}{2 c_W} \right] f \\ &= \frac{g}{c_W} \left[\bar{\nu}_L \gamma^\mu \frac{1}{2} \nu_L + \bar{e}_L \gamma^\mu \frac{2s_W^2 - 1}{2} e_L + \bar{e}_R \gamma^\mu s_W^2 e_R + \dots \right], \end{aligned} \quad (2.21)$$

⁴These expressions are consistent, up to simple redefinitions of the mixing angles, with the ones of Eq. (D5) in Ref. [75].

$$\begin{aligned}
J_X^\mu &= \sum_f \bar{f} \gamma^\mu \frac{c_W g_X Q_X^f - g \epsilon Q_Y^f s_W}{2\sqrt{1-\epsilon^2} c_W} f \\
&= \frac{1}{2c_W \sqrt{1-\epsilon^2}} \left[\bar{\nu}_L \gamma^\mu (c_W g_X Q_X^{\nu L} + g \epsilon s_W) \nu_L + \bar{\nu}_R \gamma^\mu (c_W g_X Q_X^{\nu R}) \nu_R \right. \\
&\quad \left. + \bar{e}_L \gamma^\mu (c_W g_X Q_X^{eL} + g \epsilon s_W) e_L + \bar{e}_R \gamma^\mu (c_W g_X Q_X^{eR} + 2g \epsilon s_W) e_R + \dots \right]. \tag{2.22}
\end{aligned}$$

With these currents at hand, some comments are in order:

- In the limit $\alpha \rightarrow 0$, the SM is recovered.
- α contains not only the kinetic mixing ϵ but also the mass mixing δ in Eq. (2.9).
- The charged current and electromagnetic interactions are the same as in the SM.

The currents allow one to calculate physical processes, which is what will be done in the next section.

3 Neutrino-Electron Scattering in $U(1)_X$ Models

As we discussed in the previous section, neither the kinetic mixing nor the mass mixing of the gauge bosons change the charged current and electromagnetic interactions. Therefore, neutrinos still have the SM charged current with electrons and are not involved in electromagnetic interactions [64, 68]. In addition to the charged current, neutrinos can interact with electrons via Z_μ and Z'_μ . We re-emphasize that generally we refer to dark photon-like and Z' gauge bosons as simply Z' gauge bosons. The relevant interactions for neutrino-electron scattering can be written as follows:

$$\mathcal{L} \supset - (W_\mu^+ \bar{\nu} \Gamma_W^\mu \ell + \text{h.c.}) - Z_\mu (\bar{\nu} \Gamma_{\nu Z}^\mu \nu + \bar{\ell} \Gamma_{\ell Z}^\mu \ell) - Z'_\mu (\bar{\nu} \Gamma_{\nu Z'}^\mu \nu + \bar{\ell} \Gamma_{\ell Z'}^\mu \ell), \tag{3.1}$$

where

$$\Gamma_W^\mu = \gamma^\mu \frac{g}{\sqrt{2}} P_L, \tag{3.2}$$

$$\Gamma_{\nu Z}^\mu = \gamma^\mu \left[\frac{P_L}{2c_W} g c_\alpha - \frac{g \epsilon P_L s_W s_\alpha}{2c_W \sqrt{1-\epsilon^2}} - g_X s_\alpha \frac{P_\nu}{4\sqrt{1-\epsilon^2}} \right], \tag{3.3}$$

$$\Gamma_{\ell Z}^\mu = \gamma^\mu \left[\frac{2s_W^2 - P_L}{2c_W} g c_\alpha - \frac{g(3+\gamma^5) \epsilon s_W s_\alpha}{4\sqrt{1-\epsilon^2} c_W} - g_X s_\alpha \frac{P_\ell}{4\sqrt{1-\epsilon^2}} \right], \tag{3.4}$$

$$\Gamma_{\nu Z'}^\mu = \gamma^\mu \left[\frac{P_L}{2c_W} g s_\alpha + \frac{g \epsilon P_L s_W c_\alpha}{2c_W \sqrt{1-\epsilon^2}} + g_X c_\alpha \frac{P_\nu}{4\sqrt{1-\epsilon^2}} \right], \tag{3.5}$$

$$\Gamma_{\ell Z'}^\mu = \gamma^\mu \left[\frac{2s_W^2 - P_L}{2c_W} g s_\alpha + \frac{g(3+\gamma^5) \epsilon s_W c_\alpha}{4\sqrt{1-\epsilon^2} c_W} + g_X c_\alpha \frac{P_\ell}{4\sqrt{1-\epsilon^2}} \right], \tag{3.6}$$

$$P_\nu \equiv Q_{X\nu}^{R+L} + Q_{X\nu}^{R-L} \gamma^5, \tag{3.7}$$

$$P_\ell \equiv Q_{X\ell}^{R+L} + Q_{X\ell}^{R-L} \gamma^5. \tag{3.8}$$

Table 1. Anomaly free charge assignments in $U(1)_X$ models [75]. Those were designed to explain neutrino masses via the seesaw mechanism and address the flavor problem in two Higgs doublet models.

$U(1)_X$ charges	$U(1)_C$	$U(1)_D$	$U(1)_E$	$U(1)_F$	$U(1)_G$	$U(1)_{B-L}$
$\ell_L = \begin{pmatrix} \nu_L \\ e_L \end{pmatrix}$	3/4	-3/2	-3/2	-3	-1/2	-1
e_R	0	-2	-1	-4	0	-1

Here we have used $Q_X^{R\pm L} \equiv Q_X^R \pm Q_X^L$ for short.

We note that even though $Q_{X\nu}^R$ appears in the above interactions, it will disappear in the cross sections of neutrino-electron scattering because for realistic neutrino sources, neutrinos are always produced via the charged current, which means the sources only emit left-handed neutrinos (or right-handed antineutrinos). From Eq. (3.1), one can see that left-handed neutrinos can not be converted to right-handed neutrinos in any of the vertices. Therefore right-handed neutrinos are irrelevant to neutrino-electron scattering.

So far the discussion was general. In explicit UV-complete and self-consistent models the $U(1)_X$ charges should take specific values to guarantee anomaly cancellation. In this work, we will adopt the anomaly free charge assignments as listed in Tab 1. The models are adopted from Ref. [75], where they were studied in the context of two Higgs doublet models without tree-level flavor changing neutral currents. They are characteristic for many of the available $U(1)_X$ models in the literature, and can serve as benchmark models for our study.

We compute the cross sections of neutrino-electron scattering in the appendix. The results are:

$$\frac{d\sigma}{dT}(\bar{\nu} + e^- \rightarrow \bar{\nu} + e^-) = \frac{m_e G_F^2}{4\pi} \left[g_1^2 + g_2^2 \left(1 - \frac{T}{E_\nu}\right)^2 - g_1 g_2 \frac{m_e T}{E_\nu^2} \right], \quad (3.9)$$

$$\frac{d\sigma}{dT}(\nu + e^- \rightarrow \nu + e^-) = \frac{m_e G_F^2}{4\pi} \left[g_2^2 + g_1^2 \left(1 - \frac{T}{E_\nu}\right)^2 - g_1 g_2 \frac{m_e T}{E_\nu^2} \right], \quad (3.10)$$

where E_ν and T are the neutrino energy and electron recoil energy respectively, and $g_{1,2}$ are two dimensionless quantities with quite complicated expressions. They can be decomposed into several parts, to be discussed below. Eq. (3.9) or Eq. (3.10) assume that the initial neutrinos are left-handed neutrinos or right-handed antineutrinos, respectively. As one may notice, the difference between the two cross sections is simply an interchange between g_1 and g_2 ,

$$(\nu \leftrightarrow \bar{\nu}) \iff (g_1 \leftrightarrow g_2). \quad (3.11)$$

Eqs. (3.9) and (3.10) can be used for both electron neutrinos and muon neutrinos. For electron neutrinos, additional charged current contributions should be taken into account, which changes the

SM part of g_1 and g_2 .

Next we discuss the two dimensionless quantities $g_{1,2}$. They can be decomposed into three parts, referred to as the SM part $g_{1,2}^{\text{SM}}$, the new Z_μ -mediated part $a_{1,2}$ (see below), and the Z'_μ -mediated part $b_{1,2} r$:

$$g_{1,2} = g_{1,2}^{\text{SM}} + a_{1,2} + b_{1,2} r. \quad (3.12)$$

The explicit expressions of $g_{1,2}^{\text{SM}}$ depend on whether the charged current contributions should be taken into account:

$$g_1^{\text{SM}} = -2\sqrt{2}s_W^2 c_\alpha^2, \quad g_2^{\text{SM}} = \sqrt{2}c_\alpha^2 (1 - 2s_W^2) + \begin{cases} -2\sqrt{2} & \text{(neutral current + charged current)} \\ 0 & \text{(NC only)} \end{cases}. \quad (3.13)$$

The Z'_μ -mediated part $b_{1,2} r$ can change drastically for very light Z'_μ , this is quantified by the parameter r defined as

$$r \equiv \frac{1}{(2m_e T + m_{Z'}^2) G_F}. \quad (3.14)$$

For example, if $m_{Z'}$ is below 2 MeV, then in reactor neutrino scattering experiments such as TEXONO, r reaches $\mathcal{O}(10^{10})$ —see Tab. 2. Since the $m_{Z'}$ dependence of the cross section enters only via Eq. (3.14), we can thus conclude that if $2m_e T \gg m_{Z'}^2$, the experiment is insensitive to the mass of the Z'_μ . In other words, any neutrino-electron scattering experiment with a recoil energy detection threshold T_{min} should have a threshold of mass sensitivity approximately at

$$m_{Z'}^{\text{min}} \equiv \sqrt{2m_e T_{\text{min}}}. \quad (3.15)$$

Hence, if we observe a potential Z' signal much below $m_{Z'}^{\text{min}}$, the overall effect will be independent of its mass.

We shall now turn our attention to the quantities $a_{1,2}$ and $b_{1,2}$. They are small if the gauge coupling g_X , the kinetic mixing ϵ and the mass mixing s_α are small as well, i.e.

$$(a_1, a_2, b_1, b_2) \sim \mathcal{O}(s_\alpha, g_X, \epsilon)^2. \quad (3.16)$$

Without assuming any of them to be small, the exact expressions are computed in the appendix and summarized below:

$$a_1 = s_\alpha^2 \left(g_X^2 \frac{\sqrt{2}c_W^2 Q_\nu^L Q_\ell^R}{g^2(\epsilon^2 - 1)} + \epsilon g_X \frac{\sqrt{2}s_W c_W (2Q_\nu^L + Q_\ell^R)}{g(\epsilon^2 - 1)} + \epsilon^2 \frac{2\sqrt{2}s_W^2}{\epsilon^2 - 1} \right) + c_\alpha s_\alpha \left(-g_X \frac{\sqrt{2}\sqrt{1 - \epsilon^2} c_W (2s_W^2 Q_\nu^L + Q_\ell^R)}{g(\epsilon^2 - 1)} - \epsilon \frac{2\sqrt{2}\sqrt{1 - \epsilon^2} s_W (s_W^2 + 1)}{\epsilon^2 - 1} \right), \quad (3.17)$$

$$\begin{aligned}
a_2 = s_\alpha^2 & \left(g_X^2 \frac{\sqrt{2}c_W^2 Q_\nu^L Q_\ell^L}{g^2(\epsilon^2 - 1)} + \epsilon g_X \frac{\sqrt{2}c_W s_W (Q_\ell^L + Q_\nu^L)}{g(\epsilon^2 - 1)} + \epsilon^2 \frac{\sqrt{2}s_W^2}{\epsilon^2 - 1} \right) \\
& + c_\alpha s_\alpha \left(-g_X \frac{\sqrt{2}\sqrt{1 - \epsilon^2}c_W [(2s_W^2 - 1)Q_\nu^L + Q_\ell^L]}{g(\epsilon^2 - 1)} - \epsilon \frac{2\sqrt{2}\sqrt{1 - \epsilon^2}s_W^3}{\epsilon^2 - 1} \right), \tag{3.18}
\end{aligned}$$

$$\begin{aligned}
b_1 = c_\alpha^2 & \left(\frac{g^2 \epsilon^2 s_W^2}{2(\epsilon^2 - 1)c_W^2} + \frac{g\epsilon g_X s_W Q_\nu^L}{2(\epsilon^2 - 1)c_W} + \frac{g\epsilon g_X s_W Q_\ell^R}{4(\epsilon^2 - 1)c_W} + \frac{g_X^2 Q_\nu^L Q_\ell^R}{4(\epsilon^2 - 1)} \right) \\
& + c_\alpha s_\alpha \left(\epsilon \frac{g^2 \sqrt{1 - \epsilon^2} s_W (s_W^2 + 1)}{2(\epsilon^2 - 1)c_W^2} + g_X \frac{g\sqrt{1 - \epsilon^2} (2s_W^2 Q_\nu^L + Q_\ell^R)}{4(\epsilon^2 - 1)c_W} \right) \\
& + s_\alpha^2 \left(-\frac{g^2 s_W^2}{2c_W^2} \right), \tag{3.19}
\end{aligned}$$

$$\begin{aligned}
b_2 = c_\alpha^2 & \left(\epsilon^2 \frac{g^2 s_W^2}{4(\epsilon^2 - 1)c_W^2} + g_X \epsilon \frac{g s_W (Q_\ell^L + Q_\nu^L)}{4(\epsilon^2 - 1)c_W} + g_X^2 \frac{Q_\nu^L Q_\ell^L}{4(\epsilon^2 - 1)} \right) \\
& + c_\alpha s_\alpha \left(-\epsilon \frac{g^2 s_W^3}{2\sqrt{1 - \epsilon^2}c_W^2} - g_X \frac{g [(2s_W^2 - 1)Q_\nu^L + Q_\ell^L]}{4\sqrt{1 - \epsilon^2}c_W} \right) \\
& + s_\alpha^2 \left(\frac{g^2(1 - 2s_W^2)}{4c_W^2} \right). \tag{3.20}
\end{aligned}$$

The interpretation of those terms is straightforward. The terms $a_{1,2}$ contain contributions proportional to $\sin^2 \alpha$ and $\sin \alpha \cos \alpha$. Those take into account the mixing of the SM Z with the new Z' , and would disappear if the mass and kinetic mixing terms would both vanish, $\epsilon = \delta = 0$, see Eq. (2.14). The would-be SM Z boson has an admixture of the new gauge bosons and its coupling with neutrinos and electrons is modified accordingly. In analogy the terms $b_{1,2}$ contain contributions proportional to $\cos^2 \alpha$, $\sin \alpha \cos \alpha$ and $\sin^2 \alpha$. Those correspond to the coupling of the original \hat{X} boson with neutrinos and electrons, modified by its mixing with the SM Z -boson. In the limit of no mixing ($\epsilon = \delta = 0$), they would be given by $g_X^2 Q_\nu^L Q_\ell^R / 4$ and $g_X^2 Q_\nu^L Q_\ell^L / 4$, respectively. Notice that the relevant parameters a_1, a_2, b_1, b_2 have terms proportional to $\epsilon^2 g^2, g_X \epsilon, g_X^2, \epsilon g^2, g_X g$ etc. They have sometimes opposite signs, inducing interference effects which might be relevant depending on the values adopted for the parameters in a model [68]. The expressions above are exact and general. Thus the reader can easily reproduce our results and cast limits on any $U(1)_X$ model of interest.

4 Data Fitting

In this section, we use neutrino-electron scattering data to constrain $U(1)_X$ models and discuss the relevance of the Z' mass to our reasoning. It turns out that the best limits can be obtained from

reactor experiments TEXONO and GEMMA, and from the high energy beam experiment CHARM-II⁵

Heavy Z' : for Z' 's masses larger than 1.5 GeV, the effect of the Z' is negligible for all considered neutrino-electron scattering experiments. Thus, the constraints can be described in terms of dimension-6 Fermi interactions. That said, the strongest constraint in this case should come from the experiment with the best measurement of electroweak parameters (e.g. $\sin^2 \theta_W$), which happens to be the CHARM-II experiment [78, 79].

Light Z' : For Z' 's lighter than 400 keV, the energy threshold of the detector dictates its sensitivity. The GEMMA experiment has a very low threshold for measuring the electron recoil energy and for this reason is expected to impose the best constraints on very light gauge bosons [80, 81].

Intermediate Mass Z' : For gauge bosons masses between 400 keV and 1.5 GeV the interplay between precision and energy threshold takes place, encompassing experiments such as TEXONO, LSND, and Borexino, etc. In this paper, we select three sets of data: GEMMA, TEXONO and CHARM-II, which should be quite representative of all neutrino-electron scattering data at various energy scales. Actually a previous study [68] shows that for the $U(1)_{B-L}$ model, the strongest constraint on the gauge coupling mainly comes indeed from these three experiments. Including other experiments such as LSND and Borexino has little effect on the combined constraint.

The details of the data relevant to our analyses are given next.

- CHARM-II.

The CHARM-II experiment [78, 79] used a horn focused ν_μ (and $\bar{\nu}_\mu$) beam produced by the Super Proton Synchrotron (SPS) at CERN. The mean neutrino energy $\langle E_\nu \rangle$ is 23.7 GeV for ν_μ and 19.1 GeV for $\bar{\nu}_\mu$. From 1987 to 1991, 2677 ± 82 $\nu_\mu e^-$ and 2752 ± 88 $\bar{\nu}_\mu e^-$ scattering events were detected, producing a very accurate measurement of the Weinberg angle $\sin^2 \theta_W = 0.2324 \pm 0.0083$. We take the data from [78] which published the measurement of the differential cross sections (in its Tab. 2). We thus directly use the cross section data to evaluate the χ^2 -values

$$\chi_{\text{CHARM-II}}^2 = \sum_i \left(\frac{S_i - S_{i0}}{\Delta S_i} \right)^2, \quad (4.1)$$

where S_i/S_{i0} are the theoretical/measured differential cross sections, and ΔS_i is the uncertainty. Neutrino and antineutrino data are combined together in the data fitting.

⁵In the foreseeable future, limits from neutrino-electron scattering will be the leading ones. In case reactor experiments measuring coherent elastic neutrino-nucleus can improve the threshold of their detectors to currently unrealistic values (10 eV instead of present state-of-the-art 1 keV), limits obtainable by those experiments (see [76, 77]) would be of the same order of magnitude as the ones presented here.

Table 2. Configurations of neutrino-electron scattering experiments. The last two columns for $m_{Z'}^{\min}$ and r shows the threshold of the $m_{Z'}$ sensitivity [cf. Eqs. (3.15)] and the enhancement factor for a light Z' [cf. Eq. (3.14)]

source	E_ν	T	$\Delta\sigma/\sigma^{\text{SM}}$	$m_{Z'}^{\min}$	r (@ $m_{Z'} = 0$)
TEXONO (reactor $\bar{\nu}_e$)	3-8 MeV	3-8 MeV	20%	~ 2 MeV	$\sim 10^{10}$
CHARM-II (accel. $\nu_\mu + \bar{\nu}_\mu$)	~ 20 GeV	3-24 GeV	3%	~ 50 MeV	$\sim 10^7$
GEMMA (reactor $\bar{\nu}_e$)	0-8 MeV	3-25 keV	-*	~ 0.05 MeV	$\sim 10^{13}$

* The SM signal has not been observed in GEMMA.

• TEXONO

The TEXONO experiment [82] measured the $\bar{\nu}_e e^-$ cross section with a CsI(Tl) scintillating crystal detector setting near the Kuo-Sheng Nuclear Power Reactor. Therefore the neutrino flux is the standard reactor $\bar{\nu}_e$ flux which peaks around 1 MeV. However, in TEXONO events are selected in the range $3 \text{ MeV} < T < 8 \text{ MeV}$ so the low energy part ($E_\nu < 3 \text{ MeV}$) in the flux does not contribute to the signal. After data collection from 2003 to 2008, $414 \pm 80 \pm 61$ events were selected. The measured Weinberg angle is $\sin^2 \theta_W = 0.251 \pm 0.031(\text{stat}) \pm 0.024(\text{sys})$, and the ratio of experimental to SM cross section is $1.08 \pm 0.21(\text{stat}) \pm 0.16(\text{sys})$. We perform a χ^2 -fit on the measured event rate R ,

$$\chi_{\text{TEXONO}}^2 = \sum_i \left(\frac{R_i - R_i^0}{\Delta R_i} \right)^2, \quad (4.2)$$

where R_i and R_i^0 are the theoretical and measured even rates in the i -th recoil energy bin, and ΔR_i is the corresponding uncertainty. Both R_i^0 and ΔR_i can be read off from Fig. 16 of [82]. The theoretical event rate is proportional to the event numbers divided by the bin width. The event number in the recoil energy bin $T_1 < T < T_2$ is computed by,

$$N(T_1, T_2) = a \int \Phi(E_\nu) \sigma(E_\nu, \bar{T}_1, \bar{T}_2) dE_\nu. \quad (4.3)$$

Here a is an overall factor which can be calibrated using the SM values in Fig. 16 of [82], $\Phi(E_\nu)$ is the reactor neutrino flux, and σ is a partial cross section defined as

$$\sigma(E_\nu, T_1, T_2) \equiv \int_{T_1}^{T_2} \frac{d\sigma}{dT}(E_\nu, T) dT. \quad (4.4)$$

The integral can be analytically computed and the explicit expression is given in appendix C, which is technically useful in the data fitting. Note that for a neutrino of energy E_ν , the recoil energy can not exceed

$$T_{\max} = \frac{2E_\nu^2}{M + 2E_\nu}. \quad (4.5)$$

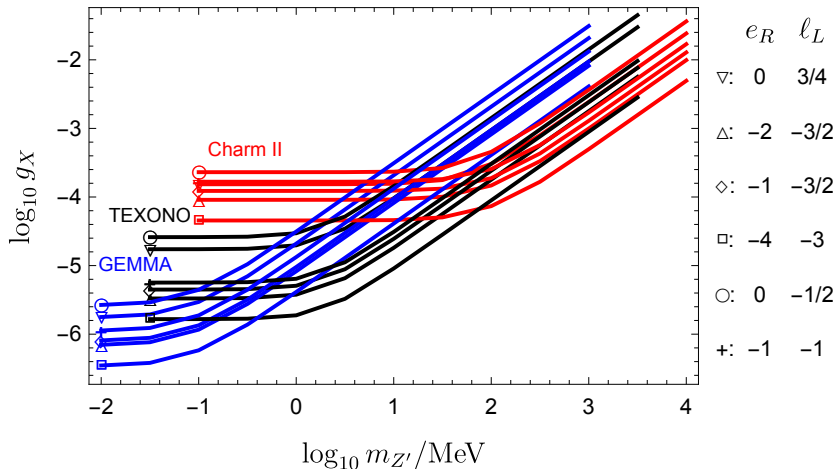


Figure 1. Constraints on g_X when $\alpha = \epsilon = 0$. The $U(1)_X$ charges of e_R and $\ell_L = (\nu_e, e)_L^T$ are listed to the right of the plot, taken from Tab. 1.

However, Eq. (4.4) does not automatically vanish if T_1 is larger than T_{\max} . Therefore in practice one should notice the technically important replacement $(T_1, T_2) \rightarrow (\bar{T}_1, \bar{T}_2)$ in Eq. (4.3), where $\bar{T}_{1,2}$ are defined as

$$\bar{T}_{1,2} \equiv \min(T_{1,2}, T_{\max}). \quad (4.6)$$

- GEMMA

The GEMMA experiment [80, 81] aimed at measuring the neutrino magnetic moment by a HPGe detector setting near the Kalinin Nuclear Power Plant. To reduce the SM background, only very low recoil energy events are selected, from 3 keV to 25 keV. In this range, the SM neutrino interactions are negligibly small with respect to its current sensitivity. We take the data from Fig. 8 of [81] and compute the event numbers also according to Eq. (4.3), except that the factor a is directly computed from the electron density in Ge, and the flux is renormalized to 2.7×10^{13} events/cm²/s. The χ^2 -fit is the same as the TEXONO experiment.

5 Bounds

Now that we have described the data sets used in the analysis and the theoretical framework of $U(1)_X$ models, we can perform a χ^2 -fit to derive limits on the relevant parameters of the models, namely, ϵ (kinetic mixing parameter), g_X (gauge coupling from the $U(1)_X$ symmetry), α (parameter that encodes the kinetic and mass mixing defined in Eq. (2.14), and $m_{Z'}$ (gauge boson mass).

We will discuss now the constraints exhibited in Figs. 1-4. In Fig. 1 we show the limits on $(m_{Z'}, g_X)$ in the absence of ϵ and α contributions, i.e. for $\epsilon = \alpha = 0$, which is equivalent to not

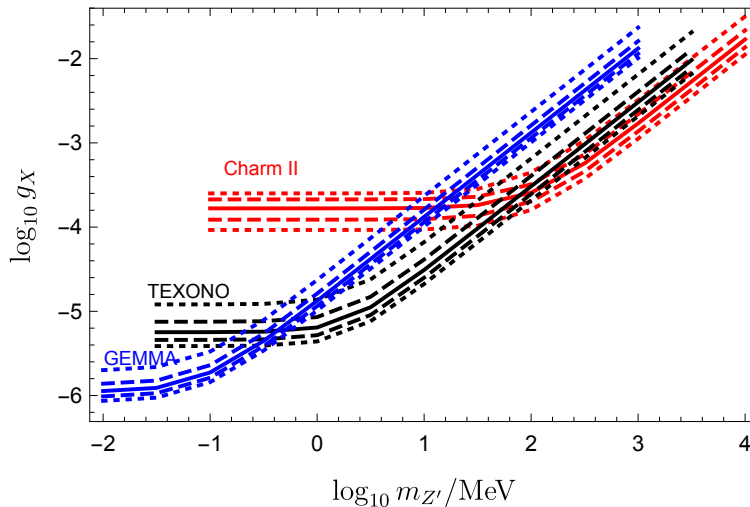


Figure 2. Constraints on g_X for $\alpha = 0.0 g_X$ (solid), $\alpha = \pm 0.5 g_X$ (dashed) and $\alpha = \pm 1.0 g_X$ (dotted), assuming $U(1)_{B-L}$ charges and $\epsilon = 0$. The bounds with negative α are lower than those with positive α .

having any kinetic and mass mixing terms. The results depend on explicit $U(1)_X$ models, i.e. the $U(1)_X$ charge assignments, which are listed in Tab. 1. Naturally, the larger the lepton charges under $U(1)_X$ the larger the new physics contribution to the neutrino-electron scattering, and thus the stronger the bound on the g_X parameter. In the $U(1)_F$ model, the left-handed leptons have charge -3 , whereas the right-handed electron has -4 . Notice that due to these large charge assignments the $U(1)_F$ is subject to the strongest bound on g_X . For $m_{Z'} < 1$ MeV, all models in our study are excluded for g_X larger than 4×10^{-6} . As for large gauge boson masses, say $m_{Z'} = 10$ GeV, $g_X > 6 \times 10^{-3}$ is excluded. The linear behavior of the limits for large Z' masses as displayed in Fig. 1 occurs simply because $m_{Z'}^2 \gg 2m_e T$, see Eq. (3.14).

Fig. 2 chooses a particular example, namely $U(1)_{B-L}$, and studies the limits on $(m_{Z'}, g_X)$ in the presence of nonzero α . We have fixed there the ratio of α and g_X to certain values. If this ratio is around 1 the situation would correspond to the VEVs of the new scalar field lying close to the electroweak scale⁶. The plot shows that within $-1 \leq \alpha/g_X \leq 1$, the bounds become stronger when α increases by roughly a factor of $10^{0.5} \approx 3$. We would like to comment that though α and g_X are two independent parameters, they can be both very small at the same order of magnitude without fine tuning. As one can see from Eq. (2.15), in the limit of $\epsilon = 0$, α is of the order δ/v^2 where v is the electroweak energy scale. If all the scalar VEVs are at (or not far from) the electroweak scale, then δ should be proportional to $g_X v^2$ [see e.g. Eq. (A.12)], thus α is at the same order of magnitude as g_X .

In Fig. 3 we present the limits on the kinetic mixing as a function of the Z' mass for $g_X = \alpha = 0$. This is an approximate case. Notice from Eq. (2.15) that if $\epsilon, \delta \ll 1$, then $\tan \alpha \sim \epsilon s_W$, or $\alpha \sim \epsilon/2$.

⁶The case of $\epsilon \sim g_X$ seems less realistic and hence we do not show a corresponding plot different values of ϵ . For $\alpha \ll g_X$ the limits are insensitive to α , for $\alpha \gg g_X$ we approach the situation displayed in Fig. 3.

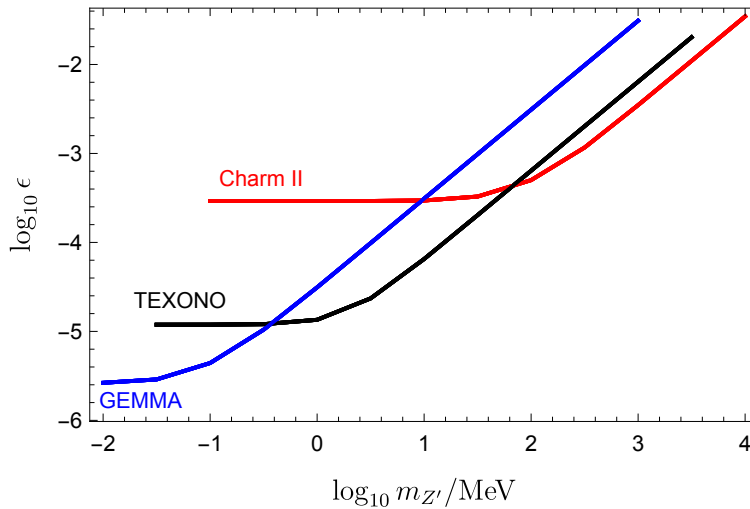


Figure 3. Constraints on ϵ when $g_X = \alpha = 0$. The result in this case is independent of the $U(1)_X$ charge assignments.

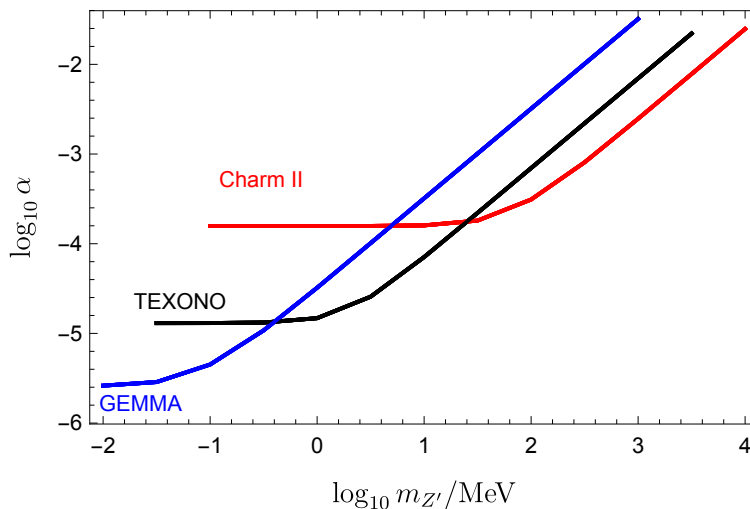


Figure 4. Constraints on α when $g_X = \epsilon = 0$. The result in this case is independent of the $U(1)_X$ charge assignments.

Thus, the choice $\alpha = 0$ as done in Fig. 3 is just an approximation. This setup is thus corresponding to a model with no mass mixing and the g_X coupling finely tuned. Anyways, as before, it is quite visible the complementary role that GEMMA, TEXONO and CHARM-II play at probing light vector mediators.

In Fig. 4, we show an orthogonal scenario, namely bounds on the parameter α as a function of Z' mass with $g_X, \epsilon = 0$. This case is relevant to a model featuring a sizable mass mixing, no

kinetic mixing and a dwindled g_X coupling. These bounds are independent of the $U(1)_X$ charges of the fermions and thus can be regarded being model-independent. We highlight that there are other relevant limits on the mass mixing parameter, such as those stemming from coherent neutrino-nucleus scattering or atomic parity violation, but they are not as restrictive as neutrino-electron scattering yet.

6 Conclusion

Additional neutral gauge bosons are a common feature of theories beyond the Standard Model. We have investigated here several different $U(1)_X$ models and have presented bounds on the key physical parameters (mass, gauge coupling and quantities describing mixing). The data we have used is from past experiments on neutrino-electron scattering, namely CHARM-II, GEMMA and TEXONO. We have provided general formulas for the Z - Z' mixing and for the cross sections that allow to use them for any model with an additional Z' boson or dark photon. Our study motivates analyses of upcoming neutrino-electron scattering data to further probe the parameter space of such models.

Acknowledgments

The authors thank Miguel Campos, Thomas Rink, Diego Cogollo, Carlos Pires, Paulo Rodrigues and Carlos Yaguna for discussions. FSQ acknowledges support from MEC, UFRN and ICTP-SAIFR FAPESP grant 2016/01343-7. WR is supported by the DFG with grant RO 2516/6-1 in the Heisenberg program.

A Gauge Boson Mass Generation

In this appendix, we discuss the mass generation of the gauge bosons from the term

$$\mathcal{L} \supset \sum_{\phi} |D_{\mu}\phi|^2,$$

where ϕ stands for all kinds of scalar fields with nonzero VEVs, denoted by $\langle\phi\rangle$.

According to the definition of D_{μ} in Eq. (2.2), the mass terms of gauge bosons should be

$$\sum_{\phi} \left| \sum_{a=1}^3 gt^a \langle\phi\rangle \hat{W}_{\mu}^a + g' \frac{Q_Y^{\phi}}{2} \langle\phi\rangle \hat{B}_{\mu} + g_X \frac{Q_X^{\phi}}{2} \langle\phi\rangle \hat{X}_{\mu} \right|^2. \quad (\text{A.1})$$

First, we consider the case that ϕ is an $SU(2)_L$ doublet. The hypercharge Q_Y^{ϕ} should be 1 or -1 to make

$$\left(\frac{\sigma_3}{2} + \frac{Q_Y^{\phi}}{2} \right) \langle\phi\rangle = 0 \quad (\text{A.2})$$

possible, which is necessary to avoid a broken $U(1)_{\text{em}}$. For $Q_Y^\phi = -1$, we can redefine $\phi \rightarrow \tilde{\phi} = i\sigma_2\phi^*$ to flip the sign of the hypercharge. So we only need to consider $Q_Y^\phi = 1$. The VEV that does not break $U(1)_{\text{em}}$ should be

$$\langle\phi\rangle = \frac{1}{\sqrt{2}} \begin{pmatrix} 0 \\ v_\phi e^{i\xi} \end{pmatrix}, \quad (\text{A.3})$$

where a complex phase ξ is allowed (e.g. in a CP violating 2 Higgs doublet model). The gauge boson mass matrix (in the fundamental basis) computed from Eqs. (A.3) and (A.1) turns out to be

$$\hat{M}^2 = \begin{pmatrix} \frac{1}{4}g^2v_\phi^2 & 0 & 0 & 0 & 0 \\ 0 & \frac{1}{4}g^2v_\phi^2 & 0 & 0 & 0 \\ 0 & 0 & \frac{1}{4}g^2v_\phi^2 & -\frac{1}{4}gv_\phi^2g' & -\frac{1}{4}gg_XQ_X^\phi v_\phi^2 \\ 0 & 0 & -\frac{1}{4}gv_\phi^2g' & \frac{1}{4}v_\phi^2g'^2 & \frac{1}{4}g_XQ_X^\phi v_\phi^2g' \\ 0 & 0 & -\frac{1}{4}gg_XQ_X^\phi v_\phi^2 & \frac{1}{4}g_XQ_X^\phi v_\phi^2g' & \frac{1}{4}g_X^2(Q_X^\phi v_\phi)^2 \end{pmatrix}. \quad (\text{A.4})$$

Next, we consider a singlet ϕ . Similar to the argument around Eq. (A.2), we get $Q_Y^\phi = 0$. The most general VEV is

$$\langle\phi\rangle = \frac{1}{\sqrt{2}}v_\phi e^{i\xi}, \quad (\text{A.5})$$

which leads to the mass matrix

$$\hat{M}^2 = \text{diag} \left(0, 0, 0, 0, \frac{1}{4}g_X^2Q_X^\phi v_\phi^2 \right). \quad (\text{A.6})$$

Therefore, for arbitrary numbers of doublet and singlet scalar fields, the mass matrix should be

$$\hat{M}^2 = \begin{pmatrix} \frac{1}{4}g^2v^2 & 0 & 0 & 0 & 0 \\ 0 & \frac{1}{4}g^2v^2 & 0 & 0 & 0 \\ 0 & 0 & \frac{1}{4}g^2v^2 & -\frac{1}{4}gg'v^2 & -\frac{1}{4}gg_Xv_X^2 \\ 0 & 0 & -\frac{1}{4}gg'v^2 & \frac{1}{4}g'^2v^2 & \frac{1}{4}g_Xg'v_X^2 \\ 0 & 0 & -\frac{1}{4}gg_Xv_X^2 & \frac{1}{4}g_Xg'v_X^2 & \frac{1}{4}g_X^2v_{XX}^2 \end{pmatrix}, \quad (\text{A.7})$$

where

$$v^2 = \sum_{\phi=\text{doublets}} v_\phi^2, \quad (\text{A.8})$$

$$v_X^2 = \sum_{\phi=\text{doublets}} v_\phi^2 Q_X^\phi, \quad (\text{A.9})$$

$$v_{XX}^2 = \sum_{\phi=\text{all}} (Q_X^\phi v_\phi)^2. \quad (\text{A.10})$$

The matrix in Eq. (A.7) can be block-diagonalized as follows,

$$\hat{M}^2 = U_W \begin{pmatrix} \frac{g^2 v^2}{4} I_{2 \times 2} & 0 & 0 & 0 \\ 0 & 0 & 0 & 0 \\ 0 & 0 & z & \delta \\ 0 & 0 & \delta & x \end{pmatrix} U_W^T, \quad (\text{A.11})$$

where

$$z \equiv \frac{1}{4} v^2 (g^2 + g'^2), \quad \delta \equiv -\frac{1}{4} g_X v_X^2 \sqrt{g^2 + g'^2}, \quad x \equiv \frac{1}{4} g_X^2 v_{XX}^2, \quad (\text{A.12})$$

$$U_W = \begin{pmatrix} I_{2 \times 2} & & & \\ & s_W & c_W & 0 \\ & c_W & -s_W & 0 \\ & 0 & 0 & 1 \end{pmatrix}, \quad (\text{A.13})$$

$$s_W = \frac{g'}{\sqrt{g^2 + g'^2}}, \quad c_W = \frac{g}{\sqrt{g^2 + g'^2}}. \quad (\text{A.14})$$

The expression for \hat{M}^2 in Eq. (A.11) is the most general mass term including mass mixing in scenarios in which $U(1)_{\text{em}}$ survives the symmetry breaking.

For completeness, we finally give the exact expressions for the physical Z and Z' boson masses, which read

$$m_Z^2 = \frac{x + z + 2\delta s_W \epsilon - c_W^2 z \epsilon^2 + \sqrt{\Delta}}{2(1 - \epsilon^2)}, \quad (\text{A.15})$$

$$m_{Z'}^2 = \frac{x + z + 2\delta s_W \epsilon - c_W^2 z \epsilon^2 - \sqrt{\Delta}}{2(1 - \epsilon^2)}, \quad (\text{A.16})$$

with

$$\Delta \equiv (1 - c_W^2 \epsilon^2) (4\delta^2 + 4\delta s_W z \epsilon + z^2 - c_W^2 z^2 \epsilon^2) + 2(1 + s_W^2) x z \epsilon^2 + 4\delta s_W x \epsilon + x^2 - 2x z. \quad (\text{A.17})$$

B Cross Sections of Neutrino-Electron Scattering

Here we present the analytical calculation of the cross sections of (anti)neutrino-electron scattering in a general $U(1)_X$ model. The relevant Feynman diagrams are presented in Fig. 5, where diagrams (a1)-(a3) are for antineutrino scattering and (b1)-(b3) are for neutrino scattering. Diagrams (a1) and (b1) are purely SM contributions, while diagrams (a3) and (b3) are new contributions due to the extra $U(1)_X$. Although (a2) and (b2) are SM diagrams they may be modified in this model due to the kinetic mixing of gauge bosons.

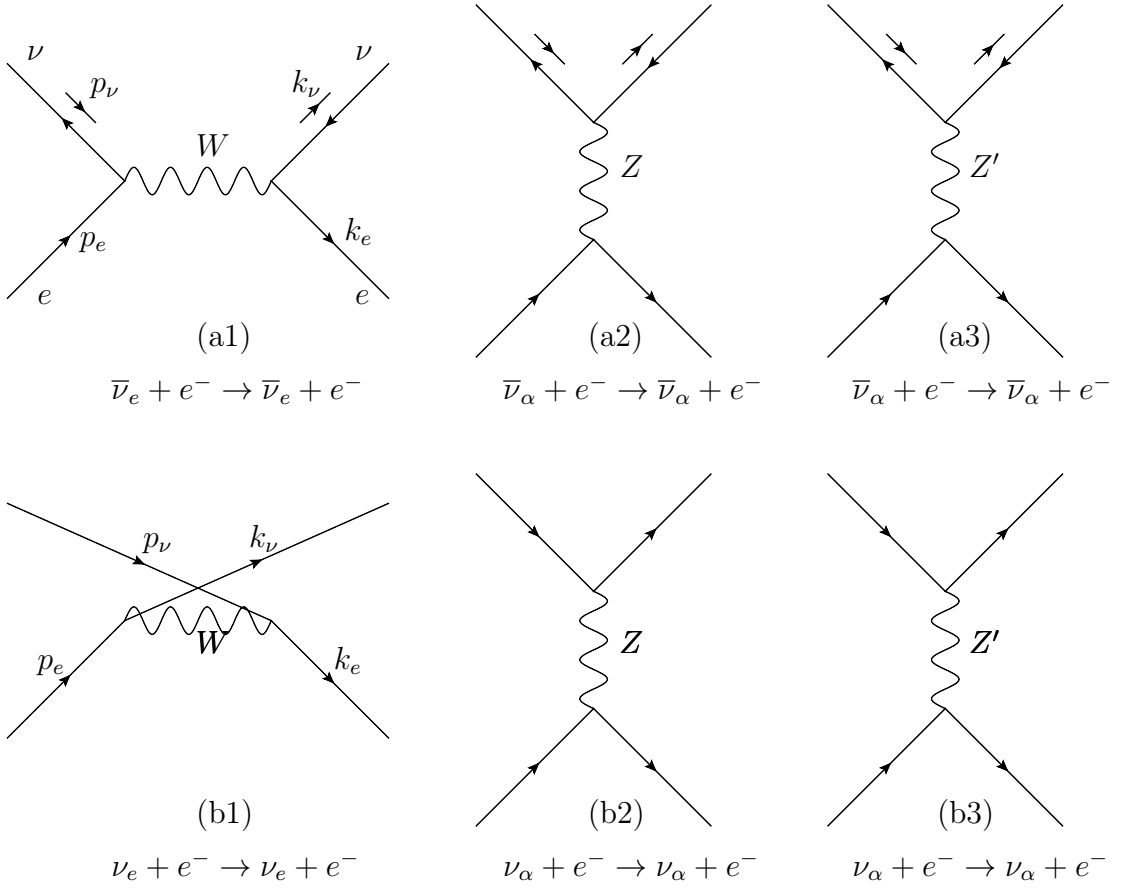


Figure 5. The Feynman diagrams of $\bar{\nu}_\alpha + e^- \rightarrow \bar{\nu}_\alpha + e^-$ (upper three diagrams) and $\nu_\alpha + e^- \rightarrow \nu_\alpha + e^-$ (lower three diagrams). The W -mediated diagrams (a1) and (b1) exist only when $\alpha = e$.

The initial/final states (momenta and spins) of neutrinos and electrons are denoted in the way shown in Fig. 5. The scattering amplitudes are written as follows:

$$i\mathcal{M}_{a1} = \bar{v}^s(p_\nu) \left(i \frac{g}{\sqrt{2}} \gamma_L^\mu \right) u^r(p_e) \frac{-i}{p_W^2 - m_W^2} \bar{u}^{r'}(k_e) \left(i \frac{g}{\sqrt{2}} \gamma_{L\mu} \right) v^{s'}(k_\nu) \quad (\text{B.1})$$

$$= \bar{v}^s(p_\nu) \left(i \frac{g}{\sqrt{2}} \gamma_L^\mu \right) v^{s'}(k_\nu) \frac{-i}{p_W^2 - m_W^2} \bar{u}^{r'}(k_e) \left(i \frac{g}{\sqrt{2}} \gamma_{L\mu} \right) u^r(p_e), \quad (\text{B.2})$$

$$i\mathcal{M}_{a2} = \bar{v}^s(p_\nu) (i\Gamma_{\nu Z})^\mu v^{s'}(k_\nu) \frac{-i}{p_Z^2 - m_Z^2} \bar{u}^{r'}(k_e) (i\Gamma_{eZ})_\mu u^r(p_e), \quad (\text{B.3})$$

$$i\mathcal{M}_{a3} = \bar{v}^s(p_\nu) (i\Gamma_{\nu Z'})^\mu v^{s'}(k_\nu) \frac{-i}{p_{Z'}^2 - m_{Z'}^2} \bar{u}^{r'}(k_e) (i\Gamma_{eZ'})_\mu u^r(p_e), \quad (\text{B.4})$$

$$i\mathcal{M}_{b1} = \bar{u}^{s'}(k_\nu) \left(i \frac{g}{\sqrt{2}} \gamma_L^\mu \right) u^r(p_e) \frac{-i}{p_W^2 - m_W^2} \bar{u}^{r'}(k_e) \left(i \frac{g}{\sqrt{2}} \gamma_{L\mu} \right) u^s(p_\nu), \quad (\text{B.5})$$

$$= \bar{u}^{s'}(k_\nu) \left(i \frac{g}{\sqrt{2}} \gamma_L^\mu \right) u^s(p_\nu) \frac{-i}{p_W^2 - m_W^2} \bar{u}^{r'}(k_e) \left(i \frac{g}{\sqrt{2}} \gamma_{L\mu} \right) u^r(p_e), \quad (\text{B.6})$$

$$i\mathcal{M}_{b2} = \bar{u}^{s'}(k_\nu) (i\Gamma_{\nu Z})^\mu u^s(p_\nu) \frac{-i}{p_Z^2 - m_Z^2} \bar{u}^{r'}(k_e) (i\Gamma_{\ell Z})_\mu u^r(p_e), \quad (\text{B.7})$$

$$i\mathcal{M}_{b3} = \bar{u}^{s'}(k_\nu) (i\Gamma_{\nu Z'})^\mu u^s(p_\nu) \frac{-i}{p_{Z'}^2 - m_{Z'}^2} \bar{u}^{r'}(k_e) (i\Gamma_{\ell Z'})_\mu u^r(p_e) \quad (\text{B.8})$$

where

$$\gamma_L^\mu \equiv \gamma^\mu \frac{1 - \gamma^5}{2} = \frac{1 + \gamma^5}{2} \gamma^\mu, \quad (\text{B.9})$$

$$p_W = p_\nu + p_e, \text{ (for } \bar{\nu}) \text{ or } p_e - k_\nu, \text{ (for } \nu), \quad (\text{B.10})$$

$$p_Z = p_{Z'} = p_\nu - k_\nu. \quad (\text{B.11})$$

In the second lines of $i\mathcal{M}_{a1}$ and $i\mathcal{M}_{b1}$, we have applied Fierz transformation to get uniform expressions so that they can be combined with the NC contributions.

The total amplitudes of $\bar{\nu}_e + e^-$ scattering and $\nu_e + e^-$ scattering are

$$i\mathcal{M}_a \equiv \sum_j i\mathcal{M}_{aj} = \sum_j \bar{v}^s(p_\nu) P_R (\Gamma_j)^\mu v^{s'}(k_\nu) \bar{u}^{r'}(k_e) i \left(\tilde{\Gamma}_j \right)_\mu u^r(p_e), \quad (\text{B.12})$$

$$i\mathcal{M}_b \equiv \sum_j i\mathcal{M}_{bj} = \sum_j \bar{u}^{s'}(k_\nu) (\Gamma_j)^\mu P_L u^s(p_\nu) \bar{u}^{r'}(k_e) i \left(\tilde{\Gamma}_j \right)_\mu u^r(p_e), \quad (\text{B.13})$$

where

$$(\Gamma_1, \Gamma_2, \Gamma_3) \equiv \left(\frac{g}{\sqrt{2}} \gamma_L^\mu, \Gamma_{\nu Z}, \Gamma_{\nu Z'} \right), \quad (\text{B.14})$$

$$(\tilde{\Gamma}_1, \tilde{\Gamma}_2, \tilde{\Gamma}_3) \equiv \left(\frac{1}{\chi_W} \frac{g}{\sqrt{2}} \gamma_L^\mu, \frac{1}{\chi_Z} \Gamma_{\ell Z}, \frac{1}{\chi_{Z'}} \Gamma_{\ell Z'} \right), \quad (\text{B.15})$$

$$\chi_W \equiv p_W^2 - m_W^2, \quad \chi_Z \equiv p_Z^2 - m_Z^2, \quad \chi_{Z'} \equiv p_{Z'}^2 - m_{Z'}^2. \quad (\text{B.16})$$

Note that in realistic experiments the incoming (anti)neutrinos should be (right-)left-handed. So in practice, one can attach the right-handed or left-handed projectors $P_R = \frac{1+\gamma^5}{2}$, $P_L = \frac{1-\gamma^5}{2}$ to the initial state of incoming antineutrinos or neutrinos respectively:

$$\bar{v}^s(p_\nu) \rightarrow \bar{v}^s(p_\nu) P_R, \quad (\text{B.17})$$

$$u^s(p_\nu) \rightarrow P_L u^s(p_\nu). \quad (\text{B.18})$$

Applying the trace technology, we get

$$\begin{aligned}
|i\mathcal{M}_a|^2 &= \sum_{ss'} \frac{1}{2} \sum_{rr'} |i\mathcal{M}_a^{ss'rr'}|^2 \\
&= \sum_{jk} \text{tr} [\gamma \cdot p_\nu P_R \Gamma_j^\mu \gamma \cdot k_\nu \Gamma_k^\rho P_L] \frac{\text{tr}}{2} [(\gamma \cdot k_e + m_e) \tilde{\Gamma}_{j\mu} (\gamma \cdot p_e + m_e) \tilde{\Gamma}_{k\rho}] \\
&= 8E_\nu^2 m_e^2 \left[G_+^2 + G_-^2 \left(1 - \frac{T}{E_\nu}\right)^2 - G_+ G_- \frac{m_e T}{E_\nu^2} \right], \tag{B.19}
\end{aligned}$$

where

$$G_\pm \equiv \sum_i (c_i - d_i) (\tilde{c}_i \pm \tilde{d}_i), \tag{B.20}$$

and c_i , d_i , \tilde{c}_i , and \tilde{d}_i are defined by

$$\Gamma_i^\mu = \gamma^\mu (c_i + d_i \gamma^5), \quad \tilde{\Gamma}_i^\mu = \gamma^\mu (\tilde{c}_i + \tilde{d}_i \gamma^5). \tag{B.21}$$

From Eqs. (B.14) and (B.15), the explicit values of c_i , d_i , \tilde{c}_i , and \tilde{d}_i are

$$\begin{aligned}
(c_1, d_1, \tilde{c}_1, \tilde{d}_1) &= \left(\frac{g}{2\sqrt{2}}, -\frac{g}{2\sqrt{2}}, \frac{g}{2\sqrt{2}\chi_W}, -\frac{g}{2\sqrt{2}\chi_W} \right), \\
c_2 &= \frac{g\sqrt{1-\epsilon^2}c_\alpha - c_W g_X s_\alpha Q_\nu^V - g\epsilon s_\alpha s_W}{4\sqrt{1-\epsilon^2}c_W}, \quad d_2 = c_2 |g \rightarrow -g, Q_\nu^V \rightarrow Q_\nu^A \\
c_3 &= \frac{c_\alpha c_W g_X Q_\nu^V + g\epsilon c_\alpha s_W + g\sqrt{1-\epsilon^2}s_\alpha}{4\sqrt{1-\epsilon^2}c_W}, \quad d_3 = c_3 |g \rightarrow -g, Q_\nu^V \rightarrow Q_\nu^A \\
\tilde{c}_2 &= -\frac{s_\alpha (c_W g_X Q_\ell^V + 3g\epsilon s_W) + c_\alpha g (1 - 4s_W^2) \sqrt{1-\epsilon^2}}{4c_W \chi_Z \sqrt{1-\epsilon^2}}, \\
\tilde{c}_3 &= \frac{c_\alpha c_W g_X Q_\ell^V + 3g\epsilon c_\alpha s_W + g s_\alpha (4s_W^2 - 1) \sqrt{1-\epsilon^2}}{4c_W \chi_{Z'} \sqrt{1-\epsilon^2}}, \\
\tilde{d}_2 &= \frac{-c_W g_X s_\alpha Q_\ell^A + g\sqrt{1-\epsilon^2}c_\alpha - g\epsilon s_\alpha s_W}{4\sqrt{1-\epsilon^2}c_W \chi_Z}, \\
\tilde{d}_3 &= \frac{c_\alpha c_W g_X Q_\ell^A + g\epsilon c_\alpha s_W + g\sqrt{1-\epsilon^2}s_\alpha}{4\sqrt{1-\epsilon^2}c_W \chi_{Z'}}.
\end{aligned}$$

One can compute $|i\mathcal{M}_b|^2$ in the similar way. The result is

$$|i\mathcal{M}_b|^2 = 8E_\nu^2 m_e^2 \left[G_-^2 + G_+^2 \left(1 - \frac{T}{E_\nu}\right)^2 - G_+ G_- \frac{m_e T}{E_\nu^2} \right]. \tag{B.22}$$

Plugging Eqs. (B.19) and (B.22) into the cross section formula

$$\frac{d\sigma}{dT} = \frac{|i\mathcal{M}|^2}{32\pi m_e E_\nu}, \quad (\text{B.23})$$

we get

$$\frac{d\sigma}{dT}(\bar{\nu}_e + e^- \rightarrow \bar{\nu}_e + e^-) = \frac{m_e}{4\pi} \left[G_+^2 + G_-^2 \left(1 - \frac{T}{E_\nu}\right)^2 - G_+ G_- \frac{m_e T}{E_\nu^2} \right], \quad (\text{B.24})$$

$$\frac{d\sigma}{dT}(\nu_e + e^- \rightarrow \nu_e + e^-) = \frac{m_e}{4\pi} \left[G_-^2 + G_+^2 \left(1 - \frac{T}{E_\nu}\right)^2 - G_+ G_- \frac{m_e T}{E_\nu^2} \right], \quad (\text{B.25})$$

where

$$G_+ = \frac{g^2 c_\alpha^2 s_W^2 + A_+ s_\alpha^2 + B_+ c_\alpha s_\alpha}{2c_W^2 \chi_Z} + \frac{g^2 s_\alpha^2 s_W^2 + A_+ c_\alpha^2 - B_+ c_\alpha s_\alpha}{2c_W^2 \chi_{Z'}}, \quad (\text{B.26})$$

$$G_- = \frac{g^2}{2\chi_W} + \frac{A_- s_\alpha^2 + B_- c_\alpha s_\alpha + g^2 c_\alpha^2 (s_W^2 - \frac{1}{2})}{2c_W^2 \chi_Z} + \frac{A_- c_\alpha^2 - B_- c_\alpha s_\alpha + g^2 s_\alpha^2 (s_W^2 - \frac{1}{2})}{2c_W^2 \chi_{Z'}}, \quad (\text{B.27})$$

$$A_+ \equiv \frac{g\epsilon c_W g_X s_W (2Q_\nu^L + Q_\ell^R) + c_W^2 g_X^2 Q_\nu^L Q_\ell^R + 2g^2 \epsilon^2 s_W^2}{2(1 - \epsilon^2)}, \quad (\text{B.28})$$

$$B_+ \equiv \frac{-g\sqrt{1 - \epsilon^2} c_W g_X (2s_W^2 Q_\nu^L + Q_\ell^R) - 2g^2 \epsilon \sqrt{1 - \epsilon^2} s_W^3 - 2g^2 \epsilon \sqrt{1 - \epsilon^2} s_W}{2(1 - \epsilon^2)}, \quad (\text{B.29})$$

$$A_- \equiv \frac{(-c_W g_X Q_\ell^L - g\epsilon s_W) (c_W g_X Q_\nu^L + g\epsilon s_W)}{2(\epsilon^2 - 1)}, \quad (\text{B.30})$$

$$B_- \equiv \frac{g\sqrt{1 - \epsilon^2} (c_W g_X (-Q_\nu^L + 2s_W^2 Q_\nu^L + Q_\ell^L) + 2g\epsilon s_W^3)}{2(\epsilon^2 - 1)}. \quad (\text{B.31})$$

So far we have not taken any approximation in the above calculation. Since most neutrino-electron scattering data are at energies much lower than m_W and m_Z , we will take the approximation

$$\chi_W \approx -\frac{\sqrt{2}g^2}{8G_F}, \quad \chi_Z \approx -\frac{\sqrt{2}g^2}{8G_F c_W^2}, \quad \chi_{Z'} = -(2m_e T + m_{Z'}^2). \quad (\text{B.32})$$

If the contribution of diagram (a1) or (b1) in Fig. 5 is absent, one simply applies the limit

$$\chi_W \rightarrow \infty. \quad (\text{B.33})$$

In the approximation given by Eq. (B.32) and Eq. (B.33), G_{\pm} can be expressed (we also assume $Q_{\nu}^L = Q_{\ell}^L$) as

$$G_+ = G_+^{\text{SM}} - \frac{2\sqrt{2}G_F(A_+s_{\alpha}^2 + B_+c_{\alpha}s_{\alpha})}{g^2} - \frac{g^2s_{\alpha}^2s_W^2 + A_+c_{\alpha}^2 - B_+c_{\alpha}s_{\alpha}}{2c_W^2(2m_eT + m_{Z'}^2)}, \quad (\text{B.34})$$

$$G_- = G_-^{\text{SM}} - \frac{2\sqrt{2}G_F(A_-s_{\alpha}^2 + B_-c_{\alpha}s_{\alpha})}{g^2} - \frac{g^2s_{\alpha}^2(s_W^2 - \frac{1}{2}) + A_-c_{\alpha}^2 - B_-c_{\alpha}s_{\alpha}}{2c_W^2(2m_eT + m_{Z'}^2)}, \quad (\text{B.35})$$

where G_+^{SM} and G_-^{SM} in the limit $\alpha \rightarrow 0$ are pure SM contributions:

$$G_+^{\text{SM}} = -2\sqrt{2}G_F s_W^2 c_{\alpha}^2, \quad G_-^{\text{SM}} = \begin{cases} \sqrt{2}G_F(c_{\alpha}^2(1 - 2s_W^2) - 2) & (\text{neutral current} + \text{charged current}) \\ \sqrt{2}G_F c_{\alpha}^2(1 - 2s_W^2) & (\text{NC only}) \end{cases}. \quad (\text{B.36})$$

Note that A_{\pm} and B_{\pm} are suppressed by ϵ and g_X :

$$\lim_{\epsilon, g_X \rightarrow 0} (A_{\pm}, B_{\pm}) = 0. \quad (\text{B.37})$$

Define

$$(a_1, b_1) \equiv \left(-2\sqrt{2}\frac{A_+s_{\alpha}^2 + B_+c_{\alpha}s_{\alpha}}{g^2}, -\frac{g^2s_{\alpha}^2s_W^2 + A_+c_{\alpha}^2 - B_+c_{\alpha}s_{\alpha}}{2c_W^2} \right), \quad (\text{B.38})$$

$$(a_2, b_2) \equiv \left(-2\sqrt{2}\frac{A_-s_{\alpha}^2 + B_-c_{\alpha}s_{\alpha}}{g^2}, -\frac{g^2s_{\alpha}^2(s_W^2 - \frac{1}{2}) + A_-c_{\alpha}^2 - B_-c_{\alpha}s_{\alpha}}{2c_W^2} \right), \quad (\text{B.39})$$

we can rewrite the cross section in the form of Eqs. (3.9), (3.10) and (3.12).

C Partial Cross Section

The partial cross section is defined as

$$\sigma(E_{\nu}, T_1, T_2) \equiv \int_{T_1}^{T_2} \frac{d\sigma}{dT}(E_{\nu}, T)dT. \quad (\text{C.1})$$

We can rewrite it as

$$\sigma(E_\nu, T_1, T_2) = G_F^2 \sum_{i,j} \int_{T_1}^{T_2} K_{ij} x_i x_j dT = G_F^2 (x^T I x), \quad (\text{C.2})$$

where I is a matrix defined as the integral of the matrix K . The matrix K and the vector x are given as follow:

$$x \equiv \begin{cases} (g_1^{\text{SM}} + a_1, g_2^{\text{SM}} + a_2, b_1, b_2) & (\text{for neutrino}) \\ (g_2^{\text{SM}} + a_2, g_1^{\text{SM}} + a_1, b_2, b_1) & (\text{for antineutrino}) \end{cases}, \quad (\text{C.3})$$

$$K_{ij} = \begin{pmatrix} \frac{(-T+E_\nu)^2 m_e}{4\pi E_\nu^2} & -\frac{T m_e^2}{4\pi E_\nu^2} & \frac{(-T+E_\nu)^2 m_e}{2\pi E_\nu^2 G_F (m_{Z'}^2 + 2T m_e)} & -\frac{T m_e^2}{4m_{Z'}^2 \pi E_\nu^2 G_F + 8\pi T E_\nu^2 G_F m_e} \\ 0 & \frac{m_e}{4\pi} & -\frac{T m_e^2}{4m_{Z'}^2 \pi E_\nu^2 G_F + 8\pi T E_\nu^2 G_F m_e} & \frac{m_e}{2m_{Z'}^2 \pi G_F + 4\pi T G_F m_e} \\ 0 & 0 & \frac{(-T+E_\nu)^2 m_e}{4\pi E_\nu^2 G_F (m_{Z'}^2 + 2T m_e)^2} & -\frac{T m_e^2}{4\pi E_\nu^2 G_F^2 (m_{Z'}^2 + 2T m_e)^2} \\ 0 & 0 & 0 & \frac{m_e}{4\pi G_F^2 (m_{Z'}^2 + 2T m_e)^2} \end{pmatrix}. \quad (\text{C.4})$$

The nonzero analytical expressions of $I_{ij} \equiv \int_{T_1}^{T_2} K_{ij} dT$ are:

$$I_{11} = -\frac{m_e (T_1 - T_2) (3E_\nu^2 - 3(T_1 + T_2) E_\nu + T_1^2 + T_2^2 + T_1 T_2)}{12\pi E_\nu^2}, \quad (\text{C.5})$$

$$I_{12} = \frac{m_e^2 (T_1 - T_2) (T_1 + T_2)}{8\pi E_\nu^2}, \quad (\text{C.6})$$

$$I_{13} = \frac{\log\left(\frac{m_{Z'}^2 + 2m_e T_2}{m_{Z'}^2 + 2m_e T_1}\right) (m_{Z'}^2 + 2E_\nu m_e)^2 + 2m_e (m_{Z'}^2 + m_e (4E_\nu - T_1 - T_2)) (T_1 - T_2)}{16\pi E_\nu^2 G_F m_e^2}, \quad (\text{C.7})$$

$$I_{22} = \frac{m_e (T_2 - T_1)}{4\pi}, \quad (\text{C.8})$$

$$I_{23} = -\frac{\tanh^{-1}\left(\frac{m_e (T_1 - T_2)}{m_{Z'}^2 + m_e (T_1 + T_2)}\right) m_{Z'}^2 + m_e (T_2 - T_1)}{8\pi E_\nu^2 G_F}, \quad (\text{C.9})$$

$$I_{24} = \frac{\log\left(\frac{m_{Z'}^2 + 2m_e T_2}{m_{Z'}^2 + 2m_e T_1}\right)}{4\pi G_F}, \quad (\text{C.10})$$

$$I_{33} = -\frac{\frac{1}{2} \log\left(\frac{m_{Z'}^2 + 2m_e T_2}{m_{Z'}^2 + 2m_e T_1}\right) (m_{Z'}^2 + 2E_\nu m_e) + \frac{m_e (T_1 - T_2) (m_{Z'}^4 + m_e (2E_\nu + T_1 + T_2) m_{Z'}^2 + 2m_e^2 (E_\nu^2 + T_1 T_2))}{(m_{Z'}^2 + 2m_e T_1) (m_{Z'}^2 + 2m_e T_2)}}{8\pi E_\nu^2 G_F^2 m_e^2}, \quad (\text{C.11})$$

$$I_{34} = -\frac{\left(\frac{1}{m_{Z'}^2 + 2m_e T_2} - \frac{1}{m_{Z'}^2 + 2m_e T_1}\right) m^2 - \log(m_{Z'}^2 + 2m_e T_1) + \log(m_{Z'}^2 + 2m_e T_2)}{16\pi E_\nu^2 G_F^2}, \quad (\text{C.12})$$

$$I_{44} = \frac{m_e (T_2 - T_1)}{4\pi G_F^2 (m_{Z'}^2 + 2m_e T_1) (m_{Z'}^2 + 2m_e T_2)}. \quad (\text{C.13})$$

References

- [1] **Particle Data Group** Collaboration, C. Patrignani *et. al.*, *Review of Particle Physics*, *Chin. Phys.* **C40** (2016), no. 10 100001.
- [2] M. Carena, A. Daleo, B. A. Dobrescu, and T. M. P. Tait, *Z' gauge bosons at the Tevatron*, *Phys. Rev.* **D70** (2004) 093009, [[hep-ph/0408098](#)].
- [3] P. Langacker, *The Physics of Heavy Z' Gauge Bosons*, *Rev. Mod. Phys.* **81** (2009) 1199–1228, [[0801.1345](#)].
- [4] P. Langacker and M. Plumacher, *Flavor changing effects in theories with a heavy Z' boson with family nonuniversal couplings*, *Phys. Rev.* **D62** (2000) 013006, [[hep-ph/0001204](#)].
- [5] M. Dittmar, A.-S. Nicollerat, and A. Djouadi, *Z-prime studies at the LHC: An Update*, *Phys. Lett.* **B583** (2004) 111–120, [[hep-ph/0307020](#)].
- [6] L. Basso, A. Belyaev, S. Moretti, and C. H. Shepherd-Themistocleous, *Phenomenology of the minimal B-L extension of the Standard model: Z' and neutrinos*, *Phys. Rev.* **D80** (2009) 055030, [[0812.4313](#)].
- [7] P. J. Fox, J. Liu, D. Tucker-Smith, and N. Weiner, *An Effective Z'*, *Phys. Rev.* **D84** (2011) 115006, [[1104.4127](#)].
- [8] A. Alves, S. Profumo, and F. S. Queiroz, *The dark Z' portal: direct, indirect and collider searches*, *JHEP* **04** (2014) 063, [[1312.5281](#)].
- [9] G. Arcadi, Y. Mambrini, M. H. G. Tytgat, and B. Zaldivar, *Invisible Z' and dark matter: LHC vs LUX constraints*, *JHEP* **03** (2014) 134, [[1401.0221](#)].
- [10] J. M. Cline, G. Dupuis, Z. Liu, and W. Xue, *The windows for kinetically mixed Z'-mediated dark matter and the galactic center gamma ray excess*, *JHEP* **08** (2014) 131, [[1405.7691](#)].
- [11] A. De Simone, G. F. Giudice, and A. Strumia, *Benchmarks for Dark Matter Searches at the LHC*, *JHEP* **06** (2014) 081, [[1402.6287](#)].
- [12] O. Buchmueller, M. J. Dolan, S. A. Malik, and C. McCabe, *Characterising dark matter searches at colliders and direct detection experiments: Vector mediators*, *JHEP* **01** (2015) 037, [[1407.8257](#)].
- [13] O. Ducu, L. Heurtier, and J. Maurer, *LHC signatures of a Z' mediator between dark matter and the SU(3) sector*, *JHEP* **03** (2016) 006, [[1509.05615](#)].
- [14] A. Alves, A. Berlin, S. Profumo, and F. S. Queiroz, *Dirac-fermionic dark matter in U(1)_X models*, *JHEP* **10** (2015) 076, [[1506.06767](#)].
- [15] M. Chala, F. Kahlhoefer, M. McCullough, G. Nardini, and K. Schmidt-Hoberg, *Constraining Dark Sectors with Monojets and Dijets*, *JHEP* **07** (2015) 089, [[1503.05916](#)].
- [16] N. Okada and S. Okada, *Z'_{BL} portal dark matter and LHC Run-2 results*, *Phys. Rev.* **D93** (2016), no. 7 075003, [[1601.07526](#)].
- [17] E. Accomando, C. Coriano, L. Delle Rose, J. Fiaschi, C. Marzo, and S. Moretti, *Z, Higgses and heavy neutrinos in U(1) models: from the LHC to the GUT scale*, *JHEP* **07** (2016) 086, [[1605.02910](#)].
- [18] I. Alikhanov and E. A. Paschos, *Searching for new light gauge bosons at e⁺e⁻ colliders*, [[1710.10131](#)].

- [19] J. Erler, P. Langacker, S. Munir, and E. Rojas, *Improved Constraints on Z-prime Bosons from Electroweak Precision Data*, *JHEP* **08** (2009) 017, [[0906.2435](#)].
- [20] R. Martinez and F. Ochoa, *Constraints on 3-3-1 models with electroweak Z pole observables and $Z\hat{A}\check{A}\check{s}$ search at the LHC*, *Phys. Rev.* **D90** (2014), no. 1 015028, [[1405.4566](#)].
- [21] A. E. Carcamo Hernandez, R. Martinez, and F. Ochoa, *Z and Z' decays with and without FCNC in 331 models*, *Phys. Rev.* **D73** (2006) 035007, [[hep-ph/0510421](#)].
- [22] R. Gauld, F. Goertz, and U. Haisch, *On minimal Z' explanations of the $B \rightarrow K^* \mu^+ \mu^-$ anomaly*, *Phys. Rev.* **D89** (2014) 015005, [[1308.1959](#)].
- [23] A. J. Buras and J. Girrbach, *Left-handed Z' and Z FCNC quark couplings facing new $b \rightarrow s \mu^+ \mu^-$ data*, *JHEP* **12** (2013) 009, [[1309.2466](#)].
- [24] M. Lindner, F. S. Queiroz, and W. Rodejohann, *Dilepton bounds on left-right symmetry at the LHC run II and neutrinoless double beta decay*, *Phys. Lett.* **B762** (2016) 190–195, [[1604.07419](#)].
- [25] P. Fayet, *Light spin 1/2 or spin 0 dark matter particles*, *Phys. Rev.* **D70** (2004) 023514, [[hep-ph/0403226](#)].
- [26] C. Bouchiat and P. Fayet, *Constraints on the parity-violating couplings of a new gauge boson*, *Phys. Lett.* **B608** (2005) 87–94, [[hep-ph/0410260](#)].
- [27] M. Pospelov, A. Ritz, and M. B. Voloshin, *Secluded WIMP Dark Matter*, *Phys. Lett.* **B662** (2008) 53–61, [[0711.4866](#)].
- [28] M. Pospelov, *Secluded U(1) below the weak scale*, *Phys. Rev.* **D80** (2009) 095002, [[0811.1030](#)].
- [29] **HADES** Collaboration, G. Agakishiev *et. al.*, *Searching a Dark Photon with HADES*, *Phys. Lett.* **B731** (2014) 265–271, [[1311.0216](#)].
- [30] **WASA-at-COSY** Collaboration, P. Adlarson *et. al.*, *Search for a dark photon in the $\pi^0 \rightarrow e^+ e^- \gamma$ decay*, *Phys. Lett.* **B726** (2013) 187–193, [[1304.0671](#)].
- [31] Z.-H. Yu, Q.-S. Yan, and P.-F. Yin, *Detecting interactions between dark matter and photons at high energy $e^+ e^-$ colliders*, *Phys. Rev.* **D88** (2013), no. 7 075015, [[1307.5740](#)].
- [32] S. N. Gninenko, *Search for MeV dark photons in a light-shining-through-walls experiment at CERN*, *Phys. Rev.* **D89** (2014), no. 7 075008, [[1308.6521](#)].
- [33] **BaBar** Collaboration, J. P. Lees *et. al.*, *Search for a Dark Photon in $e^+ e^-$ Collisions at BaBar*, *Phys. Rev. Lett.* **113** (2014), no. 20 201801, [[1406.2980](#)].
- [34] P. Arias, A. Arza, B. Dobrich, J. Gamboa, and F. Mendez, *Extracting Hidden-Photon Dark Matter From an LC-Circuit*, *Eur. Phys. J.* **C75** (2015), no. 7 310, [[1411.4986](#)].
- [35] D. Curtin, R. Essig, S. Gori, and J. Shelton, *Illuminating Dark Photons with High-Energy Colliders*, *JHEP* **02** (2015) 157, [[1412.0018](#)].
- [36] **Belle** Collaboration, I. Jaegle, *Search for the dark photon and the dark Higgs boson at Belle*, *Phys. Rev. Lett.* **114** (2015), no. 21 211801, [[1502.00084](#)].
- [37] **NA48/2** Collaboration, J. R. Batley *et. al.*, *Search for the dark photon in π^0 decays*, *Phys. Lett.* **B746** (2015) 178–185, [[1504.00607](#)].

- [38] **NA64** Collaboration, D. Banerjee *et. al.*, *Search for invisible decays of sub-GeV dark photons in missing-energy events at the CERN SPS*, *Phys. Rev. Lett.* **118** (2017), no. 1 011802, [[1610.02988](#)].
- [39] **DAMIC** Collaboration, A. Aguilar-Arevalo *et. al.*, *First Direct-Detection Constraints on eV-Scale Hidden-Photon Dark Matter with DAMIC at SNOLAB*, *Phys. Rev. Lett.* **118** (2017), no. 14 141803, [[1611.03066](#)].
- [40] G. Barello, S. Chang, C. A. Newby, and B. Ostdiek, *Don't be left in the dark: Improving LHC searches for dark photons using lepton-jet substructure*, *Phys. Rev.* **D95** (2017), no. 5 055007, [[1612.00026](#)].
- [41] **CRESST** Collaboration, G. Angloher *et. al.*, *Dark-Photon Search using Data from CRESST-II Phase 2*, *Eur. Phys. J.* **C77** (2017), no. 5 299, [[1612.07662](#)].
- [42] M. He, X.-G. He, and C.-K. Huang, *Dark Photon Search at A Circular e^+e^- Collider*, *Int. J. Mod. Phys.* **A32** (2017), no. 23n24 1750138, [[1701.08614](#)].
- [43] S. Biswas, E. Gabrielli, M. Heikinheimo, and B. Mele, *Dark-photon searches via ZH production at e^+e^- colliders*, *Phys. Rev.* **D96** (2017), no. 5 055012, [[1703.00402](#)].
- [44] **BESIII** Collaboration, M. Ablikim *et. al.*, *Dark Photon Search in the Mass Range Between 1.5 and 3.4 GeV/c²*, *Phys. Lett.* **B774** (2017) 252–257, [[1705.04265](#)].
- [45] **LHCb** Collaboration, R. Aaij *et. al.*, *Search for dark photons produced in 13 TeV pp collisions*, [[1710.02867](#)].
- [46] M. He, X.-G. He, C.-K. Huang, and G. Li, *Search for a heavy dark photon at future e^+e^- colliders*, [[1712.09095](#)].
- [47] **BaBar** Collaboration, J. P. Lees *et. al.*, *Search for Invisible Decays of a Dark Photon Produced in e^+e^- Collisions at BaBar*, *Phys. Rev. Lett.* **119** (2017), no. 13 131804, [[1702.03327](#)].
- [48] H. J. Steiner, *Experimental limit on neutrino-electron scattering*, *Phys. Rev. Lett.* **24** (1970) 746–748.
- [49] F. Reines and H. S. Gurr, *Upper limit for elastic scattering of electron anti-neutrinos by electrons*, *Phys. Rev. Lett.* **24** (1970) 1448–1452.
- [50] H. S. Gurr, F. Reines, and H. W. Sobel, *Search for anti-electron-neutrino + e- scattering*, *Phys. Rev. Lett.* **28** (1972) 1406–1409.
- [51] J. F. Wheeler and C. H. Llewellyn Smith, *Electroweak Radiative Corrections to Neutrino and Electron Scattering and the Value of $\sin^2 \theta_W$* , *Nucl. Phys.* **B208** (1982) 27. [Erratum: *Nucl. Phys.* B226,547(1983)].
- [52] **CHARM** Collaboration, J. Dorenbosch *et. al.*, *EXPERIMENTAL RESULTS ON NEUTRINO - ELECTRON SCATTERING*, *Z. Phys.* **C41** (1989) 567. [Erratum: *Z. Phys.* C51,142(1991)].
- [53] **Super-Kamiokande** Collaboration, Y. Fukuda *et. al.*, *Measurement of the solar neutrino energy spectrum using neutrino electron scattering*, *Phys. Rev. Lett.* **82** (1999) 2430–2434, [[hep-ex/9812011](#)].
- [54] J. N. Bahcall, M. Kamionkowski, and A. Sirlin, *Solar neutrinos: Radiative corrections in neutrino - electron scattering experiments*, *Phys. Rev.* **D51** (1995) 6146–6158, [[astro-ph/9502003](#)].
- [55] **LSND** Collaboration, L. B. Auerbach *et. al.*, *Measurement of electron - neutrino - electron elastic scattering*, *Phys. Rev.* **D63** (2001) 112001, [[hep-ex/0101039](#)].

- [56] O. G. Miranda, M. Maya, and R. Huerta, *Update to the neutrino - electron scattering in left-right symmetric models*, *Phys. Rev.* **D53** (1996) 1719–1720, [[hep-ph/9509335](#)].
- [57] J. Barranco, O. G. Miranda, C. A. Moura, and J. W. F. Valle, *Constraining non-standard neutrino-electron interactions*, *Phys. Rev.* **D77** (2008) 093014, [[0711.0698](#)].
- [58] A. Bolanos, O. G. Miranda, A. Palazzo, M. A. Tortola, and J. W. F. Valle, *Probing non-standard neutrino-electron interactions with solar and reactor neutrinos*, *Phys. Rev.* **D79** (2009) 113012, [[0812.4417](#)].
- [59] E. A. Garcés, O. G. Miranda, M. A. Tortola, and J. W. F. Valle, *Low-Energy Neutrino-Electron Scattering as a Standard Model Probe: The Potential of LENA as Case Study*, *Phys. Rev.* **D85** (2012) 073006, [[1112.3633](#)].
- [60] J. Billard, L. E. Strigari, and E. Figueroa-Feliciano, *Solar neutrino physics with low-threshold dark matter detectors*, *Phys. Rev.* **D91** (2015), no. 9 095023, [[1409.0050](#)].
- [61] E. Bertuzzo, F. F. Deppisch, S. Kulkarni, Y. F. Perez Gonzalez, and R. Zukanovich Funchal, *Dark Matter and Exotic Neutrino Interactions in Direct Detection Searches*, *JHEP* **04** (2017) 073, [[1701.07443](#)].
- [62] W. Rodejohann, X.-J. Xu, and C. E. Yaguna, *Distinguishing between Dirac and Majorana neutrinos in the presence of general interactions*, *JHEP* **05** (2017) 024, [[1702.05721](#)].
- [63] K. A. Kouzakov and A. I. Studenikin, *Electromagnetic interactions of neutrinos in processes of low-energy elastic neutrino-electron scattering*, [[1711.00517](#)].
- [64] R. Harnik, J. Kopp, and P. A. N. Machado, *Exploring ν Signals in Dark Matter Detectors*, *JCAP* **1207** (2012) 026, [[1202.6073](#)].
- [65] Y. Kaneta and T. Shimomura, *On the possibility of a search for the $L_\mu - L_\tau$ gauge boson at Belle-II and neutrino beam experiments*, *PTEP* **2017** (2017), no. 5 053B04, [[1701.00156](#)].
- [66] C.-H. Chen and T. Nomura, *$L_\mu - L_\tau$ gauge-boson production from lepton flavor violating τ decays at Belle II*, *Phys. Rev.* **D96** (2017), no. 9 095023, [[1704.04407](#)].
- [67] T. Araki, S. Hoshino, T. Ota, J. Sato, and T. Shimomura, *Detecting the $L_\mu - L_\tau$ gauge boson at Belle II*, *Phys. Rev.* **D95** (2017), no. 5 055006, [[1702.01497](#)].
- [68] S. Bilmis, I. Turan, T. M. Aliev, M. Deniz, L. Singh, and H. T. Wong, *Constraints on Dark Photon from Neutrino-Electron Scattering Experiments*, *Phys. Rev.* **D92** (2015), no. 3 033009, [[1502.07763](#)].
- [69] S.-F. Ge and I. M. Shoemaker, *Constraining Photon Portal Dark Matter with Texono and Coherent Data*, [[1710.10889](#)].
- [70] **nuSTORM** Collaboration, P. Kyberd *et. al.*, *nuSTORM - Neutrinos from STOREd Muons: Letter of Intent to the Fermilab Physics Advisory Committee*, [[1206.0294](#)].
- [71] J. Bian, *Measurement of Neutrino-Electron Elastic Scattering at NOvA Near Detector*, in *Meeting of the APS Division of Particles and Fields (DPF 2017) Batavia, Illinois, USA, July 31-August 4, 2017*, 2017. [[1710.03428](#)].
- [72] K. S. Babu, C. F. Kolda, and J. March-Russell, *Implications of generalized $Z - Z'$ mixing*, *Phys. Rev.* **D57** (1998) 6788–6792, [[hep-ph/9710441](#)].

- [73] J. Heeck and W. Rodejohann, *Kinetic and mass mixing with three abelian groups*, *Phys. Lett.* **B705** (2011) 369–374, [[1109.1508](#)].
- [74] B. Holdom, *Two $U(1)$'s and Epsilon Charge Shifts*, *Phys. Lett.* **166B** (1986) 196–198.
- [75] M. D. Campos, D. Cogollo, M. Lindner, T. Melo, F. S. Queiroz, and W. Rodejohann, *Neutrino Masses and Absence of Flavor Changing Interactions in the 2HDM from Gauge Principles*, *JHEP* **08** (2017) 092, [[1705.05388](#)].
- [76] B. Dutta, R. Mahapatra, L. E. Strigari, and J. W. Walker, *Sensitivity to Z -prime and nonstandard neutrino interactions from ultralow threshold neutrino-nucleus coherent scattering*, *Phys. Rev.* **D93** (2016), no. 1 013015, [[1508.07981](#)].
- [77] J. B. Dent, B. Dutta, S. Liao, J. L. Newstead, L. E. Strigari, and J. W. Walker, *Accelerator and reactor complementarity in coherent neutrino scattering*, *Phys. Rev.* **D97** (2018) 035009, [[1711.03521](#)].
- [78] **CHARM-II** Collaboration, P. Vilain *et. al.*, *Measurement of differential cross-sections for muon-neutrino electron scattering*, *Phys. Lett.* **B302** (1993) 351–355.
- [79] **CHARM-II** Collaboration, P. Vilain *et. al.*, *Precision measurement of electroweak parameters from the scattering of muon-neutrinos on electrons*, *Phys. Lett.* **B335** (1994) 246–252.
- [80] A. G. Beda, E. V. Demidova, A. S. Starostin, V. B. Brudanin, V. G. Egorov, D. V. Medvedev, M. V. Shirchenko, and T. Vylov, *GEMMA experiment: Three years of the search for the neutrino magnetic moment*, *Phys. Part. Nucl. Lett.* **7** (2010) 406–409, [[0906.1926](#)].
- [81] A. G. Beda, V. B. Brudanin, V. G. Egorov, D. V. Medvedev, V. S. Pogosov, M. V. Shirchenko, and A. S. Starostin, *Upper limit on the neutrino magnetic moment from three years of data from the GEMMA spectrometer*, [1005.2736](#).
- [82] **TEXONO** Collaboration, M. Deniz *et. al.*, *Measurement of $\text{Nu}(e)\text{-bar}$ -Electron Scattering Cross-Section with a CsI(Tl) Scintillating Crystal Array at the Kuo-Sheng Nuclear Power Reactor*, *Phys. Rev.* **D81** (2010) 072001, [[0911.1597](#)].